

AD-A251 507



AEOSR-TR-12-003-03

2

## NONLINEAR WAVES IN SOLIDS GENERATED BY IMPACT

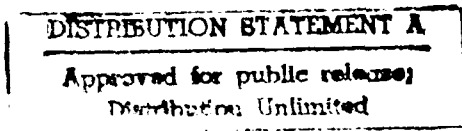
## **FINAL REPORT**

T. C. T. TING

January 27, 1992

## Air Force Office of Scientific Research

AFSOR-89-0013



**DTIC  
SELECTED  
JUN 08 1992**

**University of Illinois at Chicago  
Department of Civil Engineering, Mechanics and Metallurgy  
Box 4348, Chicago, IL 60680**

**92-14872**



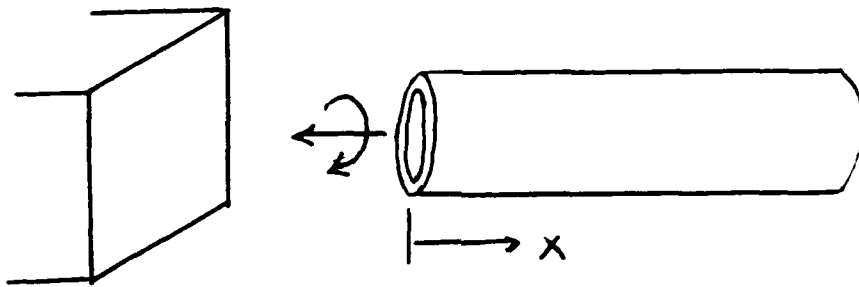
**92** 6 397

## REPORT DOCUMENTATION PAGE

1a. REPORT SECURITY CLASSIFICATION Unclassified		1b. RESTRICTIVE MARKINGS										
2a. SECURITY CLASSIFICATION AUTHORITY		3. DISTRIBUTION/AVAILABILITY OF REPORT <i>Approved for public release; distribution unlimited</i>										
2b. DECLASSIFICATION / DOWNGRADING SCHEDULE												
4. PERFORMING ORGANIZATION REPORT NUMBER(S)		5. MONITORING ORGANIZATION REPORT NUMBER(S)										
6a. NAME OF PERFORMING ORGANIZATION University of Illinois at Chicago	6b. OFFICE SYMBOL (If applicable) NA	7a. NAME OF MONITORING ORGANIZATION Air Force Office of Scientific Research										
6c. ADDRESS (City, State, and ZIP Code) CEMM Dept. (M/C246) Box 4348 Chicago, Illinois 60680		7b. ADDRESS (City, State, and ZIP Code) Bolling Air Force Base Washington, D. C. 20332										
8a. NAME OF FUNDING / SPONSORING ORGANIZATION AFSOR	8b. OFFICE SYMBOL (If applicable) NA	9. PROCUREMENT INSTRUMENT IDENTIFICATION NUMBER AFSOR-89-0013										
8c. ADDRESS (City, State, and ZIP Code) Bldg 410 Bolling AFB, DC 20332-6448		10. SOURCE OF FUNDING NUMBERS <table border="1"> <tr> <td>PROGRAM ELEMENT NO. 61102F</td> <td>PROJECT NO. 2302</td> <td>TASK NO. C2</td> <td>ASSISTING UNIT ACQUISITION NO.</td> </tr> </table>		PROGRAM ELEMENT NO. 61102F	PROJECT NO. 2302	TASK NO. C2	ASSISTING UNIT ACQUISITION NO.					
PROGRAM ELEMENT NO. 61102F	PROJECT NO. 2302	TASK NO. C2	ASSISTING UNIT ACQUISITION NO.									
11. TITLE (Include Security Classification) Nonlinear Waves in Solids Generated by Impact (U)												
12. PERSONAL AUTHOR(S) Ting, T. C. T.												
13a. TYPE OF REPORT Final	13b. TIME COVERED FROM 881015 TO 911014	14. DATE OF REPORT (Year, Month, Day) 920127	15. PAGE COUNT 9 plus									
16. SUPPLEMENTARY NOTATION												
17. COSATI CODES <table border="1"> <tr> <th>FIELD</th> <th>GROUP</th> <th>SUB-GROUP</th> </tr> <tr> <td></td> <td></td> <td></td> </tr> <tr> <td></td> <td></td> <td></td> </tr> </table>		FIELD	GROUP	SUB-GROUP							18. SUBJECT TERMS (Continue on reverse if necessary and identify by block number) Shock waves, wave curves, Riemann problems, non-strictly hyperbolic systems, conservation laws.	
FIELD	GROUP	SUB-GROUP										
19. ABSTRACT (Continue on reverse if necessary and identify by block number)  The final report summarizes contributions of research supported by the project. There are three main areas: (1) Classification of 2x2 non-strictly hyperbolic systems. (2) Wave curves with the presence of an umbilic point and an umbilic line. (3) The generalized Riemann problem. The results are of general nature that they are applicable not only to nonlinear isotropic elastic solids but also to other areas such as the oil recovery problems.												
20. DISTRIBUTION / AVAILABILITY OF ABSTRACT <input checked="" type="checkbox"/> UNCLASSIFIED/UNLIMITED <input type="checkbox"/> SAME AS RPT <input checked="" type="checkbox"/> DTIC USERS		21. ABSTRACT SECURITY CLASSIFICATION Unclassified										
22a. NAME OF RESPONSIBLE INDIVIDUAL Dr. Spencer T. Wu		22b. TELEPHONE (Include Area Code) (202) 767-6962	22c. OFFICE SYMBOL AF									

### Main contributions of the Research Project

Consider a rocket, modeled by a cylinder, rotating and moving at high speed strikes a target. It generate a longitudinal stress  $\sigma$  and torsional stress  $\tau$ .



If the material is a generally nonlinear isotropic elastic solid, the governing equations are a system of hyperbolic conservation laws

$$U_x - F(U)_t = 0 \quad (1)$$

which also arises in other physical problems such as in fluid dynamics and oil recovery problems. The function form for  $F$  may be different for other physical problems but the underlined mathematical problems are the same. Thus the results obtained from this project and from other researchers on fluid dynamics and oil recovery complement each other. The main contributions from the present project are as follows.

(1) **Classification of  $2 \times 2$  non-strictly hyperbolic system.** For fluid dynamics, Eq. (1) is a  $2 \times 2$  system. For waves in solids, it can be reduced to a  $2 \times 2$  system if the boundary conditions are prescribed in terms of stress rather on velocity. There are two wave speeds  $c_1$  and  $c_3$  and, as it happens in many applications,  $c_1 = c_3$  for certain  $U$  which is called the "umbilic" point. The system is then "non-strictly hyperbolic". Non-strictly hyperbolic systems have been the subject of intensive study by many applied mathematicians and fluid dynamicists. One of the fundamental problems for non-strictly



DIST	Special
A-1	

hyperbolic systems is the geometry of the "wave curves" near an umbilic point. The  $2 \times 2$  system can be classified according to the geometry of the wave curves near the umbilic point. For example, the wave curves for nonlinear isotropic elastic solids whose strain energy is a function of  $(\sigma, \tau)$  of order up to three, may have the geometry shown in Fig. 1

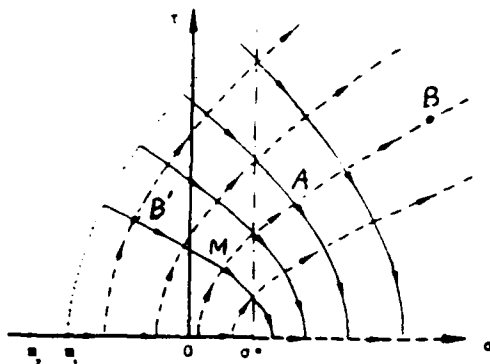


Fig. 1. Simple wave curves for Case 1:  $k \leq -1$ .

Point O is the zero stress state. If the stress is initially at point B' and the boundary condition at  $x = 0$  is at point A, the stress variation at a fix location  $x$  is, as time  $t$  increases, follows the wave curve B'MA. The corresponding wave pattern in the  $(x, t)$

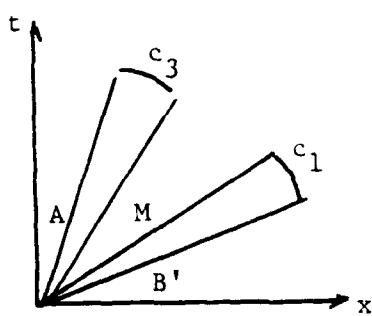


Fig. 1a

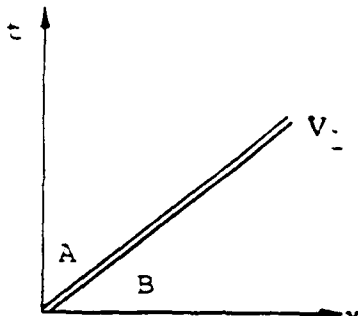


Fig. 1b

plane consists of two simple wave fans as shown in Fig 1a. In Fig. 1, the solid lines denote wave curves associated with the fast wave speed  $c_1$  and the dotted lines with the slow wave speed  $c_3$ . One can only move along the direction of the arrows and can change from a solid line to a dotted line. If the path calls for changing from a dotted curve to a solid curve or going against the direction of the arrows, a shock wave will be generated. For instance, if the initial condition is at point B and the boundary condition is at A a shock wave is generated as shown in Fig. 1b. The region before the shock wave (denoted by a double line) is the constant stress state B and the solution behind the shock wave is at A.

The point  $\sigma^*$  in Fig 1 is the umbilic point at which  $c_1 = c_3$ . Depending on the material constants, the wave curves have different geometry as shown in Figs. 2–4. Figs. 1–5 are based on the  $2 \times 2$  hyperbolic system of conservation laws. The classification of the geometry of the wave curves is one of the main contributions of this research. If the strain energy is assumed to depend on  $(\sigma, \tau)$  of order up to four, the umbilic point may not be at the  $\sigma$  axis. The wave curves near the umbilic point depend on two composite material parameters  $m$  and  $k$ . Figures 1 – 4 are special cases in which  $m = 0$ . The geometry of the wave curves near the umbilic point can be classified into five cases as shown in Fig. 5.

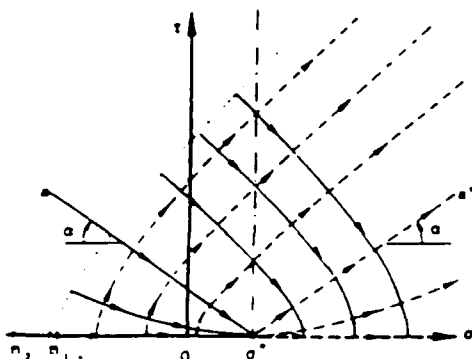


Fig. 2. Simple wave curves for Case 2:  $-1 < k \leq 0$

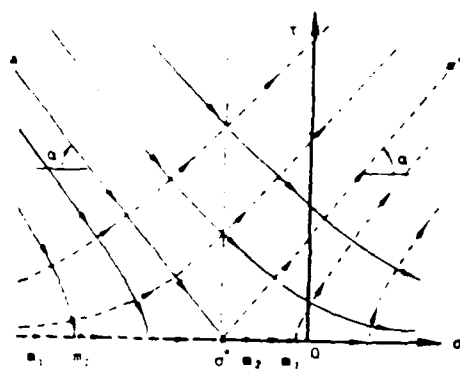


Fig. 3. Simple wave curves for Case 3:  $0 < k \leq 1$ . For Case 3a,  $m_1 > m_2 > \sigma^*$ . For Case 3b,  $m_1 < m_2 < \sigma^*$ .

#### The Riemann problem of plane waves

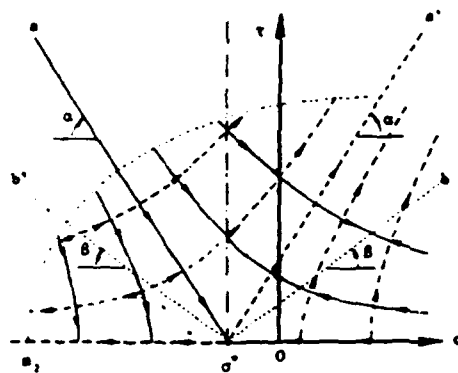


Fig. 4. Simple wave curves for Case 4a:  $1 < k \leq 2$ .

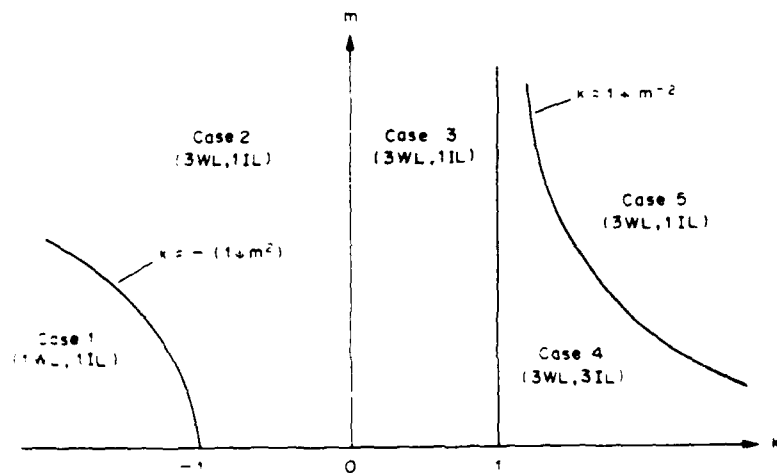


Fig. 5. Classification according to the number of wave lines (WL) and inflection lines (IL).

This classification is simpler than what is available in the literature. We did more. We classify in more detail within each case. For instance, Case 2 in Fig. 5 can be further classified as shown in Fig 6.

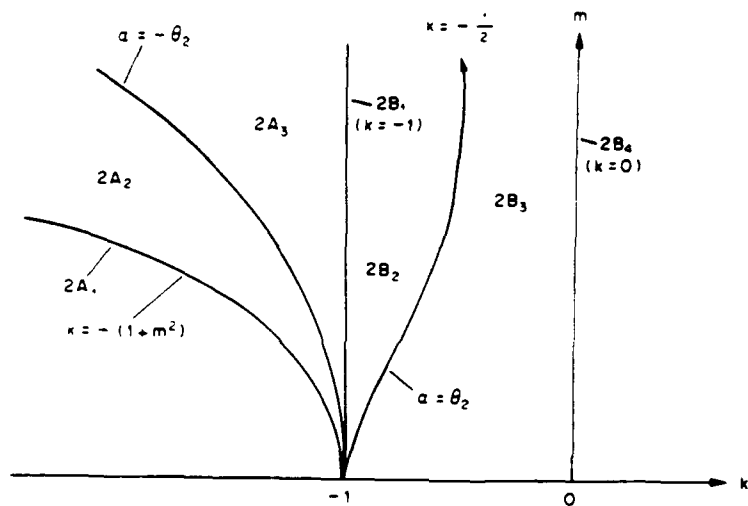


Fig. 6. Further classification of Case 2.

The geometry of wave curves in each subdivision is of course different. The implication is that, in solving the Riemann problem, it would eliminate the problem of guessing which wave curve geometry to choose for the solution.

(2). **Wave curves with the presence of an umbilic point and an umbilic line.** For the 2x2 system with the assumption that the potential function is of the third order in  $U$ , there is only one umbilic point but no umbilic line. In applications one may want to include fourth and higher order terms for a better accuracy. The system then may have more than one umbilic point and/or an umbilic line. For instance, with the fourth order term Fig. 1 is replaced by Fig. 7. Point O in Fig. 7 is the umbilic point and hence is identical to the umbilic point  $\sigma^*$  in Fig. 1. The wave curves near point O in Fig. 7 are identical to that near point  $\sigma^*$  in Fig. 1. However wave curves away from the umbilic point in the two figures are different. We have studied several potential functions of fourth

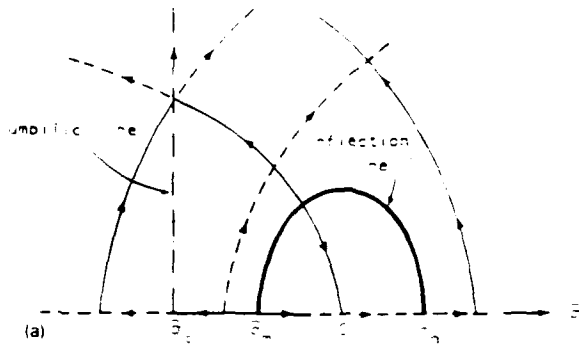


Fig. 7 Simple wave curves for Case I at  $t = 0$ ,  $-x < k < -3$   
 $1.2 \leq \sigma_1/\sigma_0 \leq 2.7$ ,  $\tau = 0$

order in  $U$  and indeed found many interesting phenomena. For instance, in Fig. 7, there is an umbilic line and also an inflection line across which the wave speed attains a maximum or a minimum. The corresponding problems in fluid dynamics do not seem to have been studied. There is no doubt that some of the results obtained are applicable to other physical problems.

(3) **Generalized Riemann problem.** The standard Riemann problem for waves in solids is that the initial conditions at  $t = 0$ ,  $x > 0$  are constant and the boundary conditions at  $x = 0$ ,  $t > 0$  are another constant. This is sometimes call the Goursat-Riemann problem. If the stress  $(\sigma, \tau)$  at  $x = 0$  after the impact is not a constant (which is the case in most practical problems) we may assume that, for small  $t$ ,

$$\sigma(0, t) = \sigma(0, 0) + \dot{\sigma} t,$$

$$\tau(0, t) = \tau(0, 0) + \dot{\tau} t,$$

where  $\dot{\sigma}, \dot{\tau}$  are constant. This is a generalized Riemann problem. It is a first order approximation in the boundary conditions. We could also consider second and higher order approximations but for the near field solutions near the impact point  $x = t = 0$ , the first order approximation is sufficient. The generalized Riemann problems have only recently

attracted the attentions of French applied mathematicians. As it turns out, our approaches in solving the generalized Riemann problem which are based on my earlier investigations on plastic waves about ten years ago, coincide with the approaches suggested by the French applied mathematicians. However, they did not apply their approaches to any physical problems. We have been studying generalized Riemann problem with applications to impact on solids in the past ten months or so. Preliminary results have been reported at a workshop on shock waves and are appearing in one of the volumes in SIAM Proceedings on Applied Mathematics. More results are being compiled and will be reported in the near future. To show the difference in the solution for the Riemann problem and for the generalized Riemann problem, consider the wave curve BA in Fig. 1 which results in a shock wave as shown in Fig. 1a. For the generalized Riemann problem, the solution is shown in Figs. 8a or 8b depending on the values of  $\sigma$ ,  $\tau$ . In Fig. 8a there is a non-steady shock wave with increasing speed and amplitude followed by a weak discontinuity along  $c_3$  characteristics. In Fig. 8b the shock wave is not affected but the region after  $c_3$  is not a constant region. It is a simple wave region.

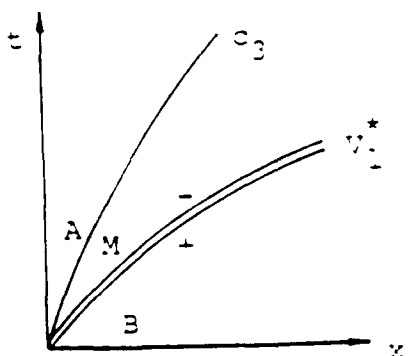


Fig. 8a

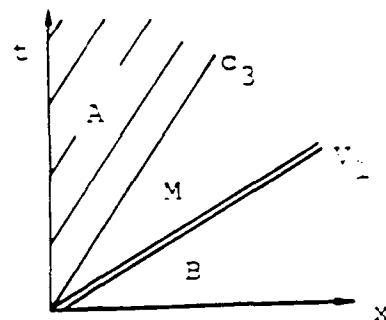


Fig. 8b

**Publications under this project.**

- [1] Guangshan Zhu and T. C. T. Ting, "Classification of 2x2 non-strictly hyperbolic systems for plane waves in isotropic elastic solids," *Int. J. Eng. Sci.* **27**, 1621–1638 (1989).
- [2] T. C. T. Ting and Tankin Wang, "The Goursat–Riemann problem for plane waves in isotropic elastic solids with velocity boundary conditions," in *Multidimensional Hyperbolic Problems and Computations. The IMA Volumes in Mathematics and Its Applications*, **29**. James Glimm and Andrew J. Majda, eds. Springer–Verlag. 367–386 (1991).
- [3] Guangshan Zhu and T. C. T. Ting, "Wave curves with the presence of an umbilic point and an umbilic line for plane waves in isotropic elastic solids," *Wave Motion*. **13**, 277–290 (1991).
- [4] Guangshan Zhu and T. C. T. Ting, "Hyperbolic conservation laws with self-similar wave curves," *Proc. Third Int. Conference on Hyperbolic Problems, Theory, Numerical Methods and Applications.* (held in Uppsala, Sweden, June 11–15, 1990.) B. Engquist and B. Gustafsson, eds. Studentlitteratur, Lund, Sweden, 1010–1024 (1991).
- [5] Tankin Wang and T. C. T. Ting, "Growth or decay of shock waves in the generalized Goursat–Riemann problem," in *Viscous Profiles and Numerical Methods for Shock Waves.* M. Shearer, ed. SIAM Proceedings Series. SIAM, Philadelphia. 161–174 (1991).
- [6] Tankin Wang and T. C. T. Ting, "The generalized Goursat–Riemann problem for plane waves in isotropic elastic solids," under preparation.

---

Copies of publications [1] and [5] are attached herewith.

## CLASSIFICATION OF $2 \times 2$ NON-STRICITLY HYPERBOLIC SYSTEMS FOR PLANE WAVES IN ISOTROPIC ELASTIC SOLIDS

GUANGSHAN ZHU and T. C. T. TING

Department of Civil Engineering, Mechanics and Metallurgy, University of Illinois at Chicago, Box 4348, Chicago, IL 60680, U.S.A.

**Abstract**—The governing equations for plane waves in generally nonlinear isotropic elastic solids are a system of  $6 \times 6$  hyperbolic conservation laws. For the half-space Riemann problem in which the initial conditions at  $t = 0$ ,  $x > 0$  and the boundary conditions at  $x = 0$ ,  $t > 0$  are constant, the system is equivalent to  $3 \times 3$  system in the full-space Riemann problem. It is further reduced to a  $2 \times 2$  system due to the fact that one of the characteristic wave speeds is linearly degenerate. For hyperelastic materials for which there exists a potential  $W$  whose gradients provide the strains, the wave curves near an isolated umbilic point are represented by the potential of the form

$$W(\sigma, \tau) = \frac{m}{3} \sigma^3 + \frac{1}{2} \sigma \tau^2 + \frac{1-k}{6} \tau^3$$

which contains two parameters  $k$  and  $m$ . The classification of the geometry of wave curves depends on the values of  $k$  and  $m$  and can be classified into five cases. The potential function considered here is equivalent to

$$W = \frac{a}{3} \sigma^3 + b \sigma^2 \tau + \sigma \tau^2$$

considered by Schaeffer and Shearer where  $a$  and  $b$  are parameters. The classification presented here seems to provide simpler algebraic expressions. It also renders more refined classification as shown in the paper.

### 1. INTRODUCTION

Consider a plane wave propagating in the  $x_1$ -direction in a fixed rectangular coordinate system  $x_1, x_2, x_3$ . The material occupies the half-space  $x_1 \geq 0$ . Let  $\sigma, \tau_2, \tau_3$  be, respectively, the normal stress and the two shear stresses on a plane  $x_1 = \text{constant}$ . If  $u, v_2, v_3$  are, respectively, the particle velocity in the  $x_1, x_2, x_3$  direction, the equations of motion and the continuity of displacements can be written as a  $6 \times 6$  system of hyperbolic conservation laws [1,2]

$$\left. \begin{aligned} \mathbf{U}_x - \mathbf{F}(\mathbf{U})_t &= \mathbf{0}, \\ \mathbf{U} &= (\sigma, \tau_2, \tau_3, u, v_2, v_3), \\ \mathbf{F}(\mathbf{U}) &= (\rho u, \rho v_2, \rho v_3, \epsilon, \gamma_2, \gamma_3). \end{aligned} \right\} \quad (1.1)$$

In the above,  $x = x_1$ ,  $t$  is the time,  $\rho$  is the mass density in the undeformed state, and  $\epsilon, \gamma_2, \gamma_3$  are, respectively, the extensional strain in the  $x_1$ -direction and the two shear strains. The constitutive equations of the material specify the relations between  $\sigma, \tau_2, \tau_3$  and  $\epsilon, \gamma_2, \gamma_3$ . For general nonlinear elastic materials for which  $\sigma, \tau_2, \tau_3$  are known functions of  $\epsilon, \gamma_2, \gamma_3$ , the system of equations (1.1) has six characteristic wave speeds  $\pm c_i, i = 1, 2, 3$  [3,4]. Without loss in generality, we let

$$0 < c_3 \leq c_2 \leq c_1.$$

The Riemann problem is a special Cauchy problem in which the initial conditions at  $t = 0$ ,  $x > 0$  and at  $t = 0$ ,  $x < 0$  are constant [1,5-9]. For plane waves in a half-space, the Riemann problem prescribes constant initial conditions at  $t = 0$ ,  $x > 0$  and constant boundary conditions at  $x = 0, t > 0$ . The solution in the  $(x, t)$  plane depends on one parameter  $x/t$  only. If the solution is continuous in  $x/t$ , we have a simple wave solution in which  $x/t = c$ , the characteristic wave speed. In particular, the stresses  $\sigma, \tau_2, \tau_3$  are continuous functions of  $c$  and, as  $c$  varies, the stresses trace out a "simple wave curve" in the stress space. Since we are considering the

half-space  $x \geq 0$ , we need only the positive wave speeds  $c_1$ ,  $c_2$ ,  $c_3$ . We therefore have three families of simple wave curves and (1.1) for the Riemann problem in the half-space is equivalent to a  $3 \times 3$  hyperbolic system.

The solution to the Riemann problem is of fundamental importance in finding the solution to a more general initial and boundary value problem [10]. The solution requires precise classification of the simple wave curves. The Riemann problem appears not only in wave propagation in solids, but also in other physical applications such as oil recovery problems [10,11] as well as in solving two-dimensional Riemann problems [12,13]. In finding the solution to the Riemann problem we need the knowledge of the geometry of simple wave curves. This leads to the classification of the hyperbolic system according to the geometry of simple wave curves. In the rest of the paper, we refer to simple wave curves as wave curves for brevity because we will not be concerned with shock wave curves.

In Section 2 we point out that when the material is isotropic, (1.1) is linearly degenerate with respect to  $c_2$ . It suffices therefore to consider wave curves associated with  $c_1$  and  $c_3$  only and (1.1) is reduced to a  $2 \times 2$  system. For hyperelastic materials for which the strains are obtainable from the gradients of potential function  $W$ , the wave curves associated with  $c_1$  and  $c_3$  are orthogonal to each other. This is presented in Section 3. The classification of the  $2 \times 2$  system is studied in Sections 4–7. For the system under consideration, there exists an umbilic point at which  $c_1 = c_3$ . The system therefore is not strictly hyperbolic [14–18]. For second order hyperelastic materials for which  $W$  can be approximated by a polynomial in stress of order up to three, there is one umbilic point which is located on the  $\sigma$ -axis. The classification of  $2 \times 2$  systems for second order materials is presented in Section 4. In Section 5 we consider the third order materials. There are now more than one umbilic point. We may also have an umbilic line. If the umbilic point is on the  $\sigma$ -axis, the classification is identical to that for the second order materials. If the umbilic point is not on the  $\sigma$ -axis, we show in Section 6 that the classification is identical to that of  $2 \times 2$  systems of general potential function near an isolated umbilic point. Section 7 contains the main results of our paper. We present the classification of  $2 \times 2$  systems of general potential function near an isolated umbilic point. The classification is different from that in [11] but can be shown to be equivalent if one rotates the coordinate axes of the stress space. The classification presented here is more refined and appears to offer simpler algebraic expressions for the boundaries between different cases.

## 2. EQUIVALENT TO $2 \times 2$ SYSTEMS FOR ISOTROPIC ELASTIC MATERIALS

When the material is isotropic, the relation

$$\tau_2/\tau_3 = \gamma_2/\gamma_3$$

holds [8]. If we let

$$\tau_2 = \tau \cos \theta, \quad \tau_3 = \tau \sin \theta, \quad \tau > 0,$$

$$\gamma_2 = \gamma \cos \theta, \quad \gamma_3 = \gamma \sin \theta, \quad \gamma > 0,$$

the rectangular coordinate system  $(\sigma, \tau_2, \tau_3)$  is transformed into a cylindrical coordinate system  $(\sigma, \tau, \theta)$ . It can be shown [8,9] that the wave curves associated with  $c_1$  and  $c_3$  are plane polarized on the  $\theta = \text{constant}$  plane. On the other hand, the wave curves associated with  $c_2$  is circularly polarized on the circle

$$\sigma = \text{constant}, \quad \tau = \text{constant}, \quad \text{for } c = c_2.$$

Moreover,  $c_2$  is a constant on the circular wave curve. Therefore  $c_2$  is linearly degenerate [10] and the  $c_2$  simple wave is in fact a shock wave. For the Riemann problem in which the initial condition and the boundary condition for  $\theta$  are different, all we have to do is to introduce a  $c_2$  shock wave which changes the value of  $\theta$  from the initial value to the value prescribed at the boundary. This is one of few special cases in nonlinear problems in which the principle of superposition applies.

It is therefore sufficient to consider  $\theta$  to be constant and the  $6 \times 6$  system of (1.1) is reduced to a  $4 \times 4$  system

$$\left. \begin{aligned} \mathbf{U}_x - \mathbf{F}(\mathbf{U})_t &= \mathbf{0}, \\ \mathbf{U} = (\sigma, \tau, u, v), \\ \mathbf{F}(\mathbf{U}) = (\rho u, \rho v, \epsilon, \gamma). \end{aligned} \right\} \quad (2.1)$$

The characteristic wave speeds  $c_1, c_3$  are the eigenvalues of the eigenrelation

$$\left. \begin{aligned} (\mathbf{I} + c\mathbf{A})\mathbf{U}' &= \mathbf{0}, \\ \mathbf{A} = \begin{bmatrix} \mathbf{0} & \rho\mathbf{I} \\ \mathbf{G} & \mathbf{0} \end{bmatrix}, \quad \mathbf{G} = \begin{bmatrix} \epsilon_\sigma & \epsilon_\tau \\ \gamma_\sigma & \gamma_\tau \end{bmatrix}. \end{aligned} \right\} \quad (2.2)$$

In the above,  $\mathbf{I}$  is a unit matrix, a prime denotes differentiation with  $c$  and the subscripts  $\sigma$  and  $\tau$  denote differentiation with these variables. Here we have assumed that the relations between  $\sigma, \tau$  and  $\epsilon, \gamma$  are invertable. If not, we limit our attention to the region where they are invertable.

Since  $\mathbf{G}$  depends on  $\sigma$  and  $\tau$  only, the four equations in (2.2), can be reduced to two equations as

$$\left. \begin{aligned} (\mathbf{G} - \eta\mathbf{I})\mathbf{s}' &= \mathbf{0}, \\ \mathbf{s} = (\sigma, \tau), \quad \eta = (\rho c^2)^{-1}. \end{aligned} \right\} \quad (2.3)$$

If we consider the  $2 \times 2$  hyperbolic system

$$\left. \begin{aligned} \mathbf{U}_t + \mathbf{F}(\mathbf{U})_x &= \mathbf{0}, \\ \mathbf{U} = (\sigma, \tau), \quad \mathbf{F}(\mathbf{U}) = (\epsilon, \gamma), \end{aligned} \right\} \quad (2.4)$$

the Riemann problem for this system also leads to (2.3). Therefore, the Riemann problem for the half-space of  $4 \times 4$  system (2.1) is equivalent to the Riemann problem for the full-space of  $2 \times 2$  system (2.4).

### 3. HYPERELASTIC MATERIALS

For hyperelastic materials there exists a potential  $W$ , the complementary strain energy [19], such that

$$\epsilon = W_\sigma, \quad \gamma = W_\tau. \quad (3.1)$$

The matrix  $\mathbf{G}$  in (2.2) has the form

$$\mathbf{G} = \begin{bmatrix} W_{\sigma\sigma} & W_{\sigma\tau} \\ W_{\sigma\tau} & W_{\tau\tau} \end{bmatrix},$$

which is symmetric. The eigenvalues  $\eta$  of  $\mathbf{G}$  are

$$\left. \begin{aligned} \eta_1 &= \frac{1}{2} \{(W_{\sigma\sigma} + W_{\tau\tau}) - \gamma\} = (\rho c_1^2)^{-1}, \\ \eta_3 &= \frac{1}{2} \{(W_{\sigma\sigma} + W_{\tau\tau}) + Y\} = (\rho c_3^2)^{-1}, \\ Y &= \{(W_{\sigma\sigma} - W_{\tau\tau})^2 + 4W_{\sigma\tau}^2\}^{1/2}. \end{aligned} \right\} \quad (3.2)$$

The eigenvector  $\mathbf{s}'$  of (2.3) provides the tangent of wave curves in the stress space  $(\sigma, \tau)$ . The differential equation for wave curves is therefore

$$\frac{\tau'}{\sigma'} = \frac{d\tau}{d\sigma} = \frac{2W_{\sigma\tau}}{(W_{\sigma\sigma} - W_{\tau\tau}) \mp Y} = \frac{-(W_{\sigma\sigma} - W_{\tau\tau}) \mp Y}{2W_{\sigma\tau}}. \quad (3.3)$$

in which the upper sign (or the lower sign) is for the  $c_1$  (or  $c_3$ ) wave curves. Due to the symmetry of  $\mathbf{G}$ , the eigenvectors associated with  $c_1$  and  $c_3$  are orthogonal to each other. This means that the wave curves for  $c_1$  and  $c_3$  are orthogonal to each other. Regarding  $z = W(\sigma, \tau)$  as a surface, it can be shown [11] that the wave curves are the projection of the lines of curvature of the surface on the  $(\sigma, \tau)$  plane.

When  $c_1 = c_3$ , i.e.,  $\eta_1 = \eta_3$ , the system is not strictly hyperbolic. The stress  $(\sigma, \tau)$  at which  $c_1 = c_3$  is called the umbilic point. We see from (3.2) that the umbilic point is located at

$$W_{\sigma\sigma} = W_{\tau\tau}, \quad W_{\sigma\tau} = 0. \quad (3.4)$$

If (3.4) are satisfied for a one-parameter family of points, we have an umbilic line. Since the umbilic line is a line of curvature of the surface  $z = W(\sigma, \tau)$ , the umbilic line is a wave curve. We also see that at the umbilic point or the umbilic line, the wave curves for  $c_1$  and  $c_3$  may not be orthogonal to each other [8,9].

The differential equation (3.3) for the wave curves has the following invariance properties:

- (i) If we multiply or divide  $W$  by a constant, (3.3) remains unchanged.
- (ii) Equation (3.3) is invariant with a translation and/or a rotation of the coordinate axes  $\sigma$  and  $\tau$  [11].
- (iii) If we expand  $W(\sigma, \tau)$  in powers of  $\sigma$  and  $\tau$ , (3.3) remains the same if we ignore the constant terms and the linear terms. It also remains the same if we ignore the term  $(\sigma^2 + \tau^2)$  because this term contributes nothing to  $W_{\sigma\sigma} - W_{\tau\tau}$  and  $W_{\sigma\tau}$  which appear in (3.3).

The above invariance properties form the bases in the sequel for reducing the potential function  $W$  to an equivalent form for classification.

#### 4. CLASSIFICATION FOR SECOND ORDER HYPERELASTIC MATERIALS

From (3.1), if the strains are to be expressed in powers of  $\sigma, \tau$  of order up to two, we have to expand  $W$  in terms of  $\sigma$  and  $\tau$  of order up to three. We may ignore the constant term in  $W$  since it contributes nothing to the strains  $\varepsilon$  and  $\gamma$ . We ignore also the first order terms in  $\sigma$  and  $\tau$  because the strains would otherwise be non-zero when the stresses are zero. Noticing that for isotropic materials  $W$  should be an even function in the shear stress  $\tau$ , we have, for the second order hyperelastic materials,

$$W(\sigma, \tau) = \frac{a}{2} \sigma^2 + \frac{d}{2} \tau^2 + \frac{b}{6} \sigma^3 + \frac{e}{2} \sigma \tau^2, \quad (4.1)$$

in which  $a, d, b, e$  are constants. From (3.1),

$$\left. \begin{aligned} \varepsilon &= a\sigma + \frac{1}{2}(b\sigma^2 + e\tau^2), \\ \gamma &= d\tau + e\sigma\tau, \end{aligned} \right\} \quad (4.2)$$

and hence  $a$  and  $d$  are the elastic constants for linear materials while  $b$  and  $e$  are the second order elastic constants. The constants  $a$  and  $d$  are related to Lamé constants  $\lambda$  and  $\mu$  by

$$a^{-1} = \lambda + 2\mu, \quad d^{-1} = \mu.$$

With  $W$  given by (4.1), the umbilic point obtained from (3.4) is located at

$$\sigma = \sigma_*, \quad \tau = 0,$$

where

$$\sigma_* = \frac{d - a}{b - e}.$$

Therefore, the umbilic point is on the  $\sigma$ -axis.

Equation (4.2) tells us that, when  $e = 0$ , the stress-strain laws for tension and shear are uncoupled. The  $2 \times 2$  system is then decoupled into two  $1 \times 1$  systems. This special case has been studied in [20]. We assume here that  $e \neq 0$ . Next, we see that if we change the sign of  $e$ , (4.1) and (4.2) remain the same if we also change the sign of  $b$ ,  $\sigma$  and  $\varepsilon$ . The wave curves for  $e < 0$  can therefore be obtained from that for  $e > 0$  by reversing the direction of the  $\sigma$ -axis and the sign of  $b$ . Hence it suffices to consider  $e > 0$ . Finally, using the invariance properties (i), (ii) and (iii) discussed in Section 4 we divide  $W$  by  $e$  and move the origin of  $(\sigma, \tau)$  plane to  $(\sigma_*, 0)$ . Equation (4.1) is then replaced by

$$W = \frac{1-k}{6} \bar{\sigma}^3 + \frac{1}{2} \bar{\sigma} \tau^2, \quad (4.3)$$

$$k = 1 - \frac{b}{e}, \quad \bar{\sigma} = \sigma - \sigma_*,$$

and the differential equation (3.3) for the wave curves can be written as

$$\frac{d\tau}{d\bar{\sigma}} = -\phi \mp (1 + \phi^2)^{1/2} = \{\phi \mp (1 + \phi^2)^{1/2}\}^{-1}, \quad (4.4)$$

$$\phi = \frac{k\bar{\sigma}}{2\tau},$$

which contains only one parameter  $k$ .

Equation (4.4) can be integrated in a closed form [21]. The wave curves have different geometry depending on the value of  $k$ . They can be classified into four cases as follows [8, 9]:

$$\left. \begin{array}{l} \text{Case 1: } k < -1. \\ \text{Case 2: } -1 \leq k \leq 0. \\ \text{Case 3: } 0 < k \leq 1. \\ \text{Case 4: } 1 < k. \end{array} \right\} \quad (4.5)$$

The geometry of wave curves for each case and the solution to the Riemann problem have been discussed in detail in [8, 9]. We will see that the classification (4.5) is a special case of the classification of general  $2 \times 2$  systems to be considered in Section 7.

## 5. CLASSIFICATION FOR THIRD ORDER HYPERELASTIC MATERIALS

We now include the third order terms in  $\sigma$  and  $\tau$  for the strains  $\varepsilon$  and  $\gamma$ . This means that  $W$  must contain the fourth order terms and we write

$$W = \frac{a}{2} \sigma^2 + \frac{d}{2} \tau^2 + \frac{b}{6} \sigma^3 + \frac{e}{2} \sigma \tau^2 + \frac{1}{12} \delta_1 \sigma^4 + \frac{1}{12} \delta_2 \tau^4 + \frac{1}{2} \delta_3 \sigma^2 \tau^2, \quad (5.1)$$

in which  $\delta_1$ ,  $\delta_2$ ,  $\delta_3$  are the third order elastic constants. The strain-stress relations (3.1) have the expressions

$$\varepsilon = a\sigma + \frac{1}{2} (b\sigma^2 + e\tau^2) + \left( \frac{1}{3} \delta_1 \sigma^2 + \delta_3 \tau^2 \right) \sigma,$$

$$\gamma = d\tau + e\sigma\tau + \left( \frac{1}{3} \delta_2 \tau^2 + \delta_3 \sigma^2 \right) \tau.$$

There are now more than one umbilic point and there may be umbilic lines. With (5.1), the conditions (3.4) for the umbilic point are

$$\left. \begin{array}{l} a + b\sigma + \delta_1 \sigma^2 + \delta_3 \tau^2 = d + e\sigma + \delta_3 \sigma^2 + \delta_2 \tau^2, \\ \tau(e + 2\delta_3 \sigma) = 0. \end{array} \right\} \quad (5.2)$$

There are several solutions to the two equations. We discuss the solutions separately below.

(A) Let  $\sigma_*^{(1)}, \sigma_*^{(2)}$  satisfy the equation

$$a + b\sigma + \delta_1\sigma^2 = d + e\sigma + \delta_3\sigma^2. \quad (5.3)$$

We then have two umbilic points at  $(\sigma_*^{(1)}, 0)$  and  $(\sigma_*^{(2)}, 0)$ . They are on the  $\sigma$ -axis. To study the geometry of wave curves near the umbilic points, we rewrite the right hand side of (5.1) in terms of  $\bar{\sigma}$  and  $\tau$  where

$$\bar{\sigma} = \sigma - \sigma_*^{(i)}, \quad i = 1, 2.$$

Using the invariance properties (ii) and (iii) and ignoring the fourth order terms, we replace (5.1) by

$$W = \frac{\bar{b}}{6} \bar{\sigma}^3 + \frac{\bar{e}}{2} \bar{\sigma}\tau^2,$$

$$\bar{b} = b + 2\delta_1\sigma_*^{(i)}, \quad \bar{e} = e + 2\delta_3\sigma_*^{(i)}.$$

Assuming that  $\bar{e} \neq 0$  and using the invariance property (i), we have

$$W = \frac{1-k}{6} \bar{\sigma}^3 + \frac{1}{2} \bar{\sigma}\tau^2, \quad k = 1 - \frac{\bar{b}}{\bar{e}}. \quad (5.4)$$

This is identical to (4.3). The geometry of wave curves near the umbilic point  $(\sigma_*^{(1)}, 0)$  or  $(\sigma_*^{(2)}, 0)$  is therefore identical to that discussed in the last section.

(B) If  $\delta_3 \neq 0$  and  $\delta_2 \neq \delta_3$ , (5.2) have the solution

$$\left. \begin{aligned} \sigma_0 &= -\frac{e}{2\delta_3}, \\ \tau_0^2 &= \frac{\{(d-a)+(e-b)\sigma_0+(\delta_3-\delta_1)\sigma_0^2\}}{(\delta_3-\delta_2)}. \end{aligned} \right\} \quad (5.5)$$

If  $\tau_0 = 0$ , the umbilic point is on the  $\sigma$ -axis and the discussion in Case (A) applies. If  $\tau_0 \neq 0$ , we have an umbilic point at  $(\sigma_0, \tau_0)$  which is not on the  $\sigma$ -axis. Let

$$\bar{\sigma} = \sigma - \sigma_0, \quad \bar{\tau} = \tau - \tau_0.$$

Using the invariance properties (ii) and (iii) and ignoring the fourth order terms we obtain

$$W = \frac{g}{6} \bar{\sigma}^3 + \frac{\bar{e}}{2} \bar{\sigma}^2 \bar{\tau} + \frac{\bar{b}}{6} \bar{\tau}^3,$$

$$g = b + 2\delta_1\sigma_0, \quad \bar{b} = 2\delta_2\tau_0, \quad \bar{e} = 2\delta_3\tau_0.$$

Since  $\bar{e} \neq 0$ , we may divide  $W$  by  $\bar{e}$  to obtain

$$W = \frac{m}{6} \bar{\sigma}^3 + \frac{1}{2} \bar{\sigma}^2 \bar{\tau} + \frac{1-k}{6} \bar{\tau}^3, \quad (5.6)$$

$$m = \frac{g}{\bar{e}}, \quad k = 1 - \frac{\bar{b}}{\bar{e}}.$$

We will show in the next section that for a general potential function  $W$  near an isolated umbilic point,  $W$  also has the expression (5.6). The classification of  $2 \times 2$  systems with  $W$  given by (5.6) is studied in Section 7.

(C) If  $\delta_2 = \delta_3 \neq 0$ , and (5.5) satisfies (5.3), we have an umbilic line at

$$\sigma_0 = -\frac{e}{2\delta_3}, \quad \tau \text{ arbitrary.}$$

This case is being studied separately in [22].

(D) If  $\delta_3 = e = 0$ , we have the umbilic line given by

$$a + b\sigma + \delta_1\sigma^3 = d + \delta_2\tau^2.$$

If  $\delta_2 \neq 0$ , the umbilic line is a parabola, hyperbola or ellipse depending on whether  $\delta_1\delta_2$  is zero, positive or negative. This case has been studied in [20]. The degenerate case  $\delta_2 = 0$  leads to two straight umbilic lines.

## 6. THE GENERAL POTENTIAL FUNCTION NEAR AN ISOLATED UMBILIC POINT

We now consider a general function  $W$  and assume that  $(\sigma_0, \tau_0)$  is an isolated umbilic point. This means, from (3.4),

$$\begin{aligned} W_{\sigma\sigma}(\sigma_0, \tau_0) &= W_{\tau\tau}(\sigma_0, \tau_0), \\ W_{\sigma\tau}(\sigma_0, \tau_0) &= 0. \end{aligned}$$

If we expand  $W$  in Taylor series at the umbilic point, use the invariance properties (ii) and (iii) and ignore the fourth order terms, we obtain

$$\begin{aligned} W &= \frac{g}{6}\bar{\sigma}^3 + \frac{e}{2}\bar{\sigma}^2\bar{\tau} + \frac{h}{2}\bar{\sigma}\bar{\tau}^2 + \frac{b}{6}\bar{\tau}^3, \\ \bar{\sigma} &= \sigma - \sigma_0, \quad \bar{\tau} = \tau - \tau_0. \end{aligned} \tag{6.1}$$

In the above,  $g$ ,  $e$ ,  $h$  and  $b$  are the third order derivatives of  $W$  at the umbilic point  $(\sigma_0, \tau_0)$ . Without loss in generality, we may assume that  $h = 0$ . If  $h \neq 0$ , we apply the invariance property (ii) by rotating the coordinate axes  $\sigma, \tau$  such that the term  $\bar{\sigma}\bar{\tau}^2$  disappears. Hence we consider

$$W = \frac{g}{6}\bar{\sigma}^3 + \frac{e}{2}\bar{\sigma}^2\bar{\tau} + \frac{b}{6}\bar{\tau}^2.$$

The special case  $e = 0$  decouples the  $2 \times 2$  system into two  $1 \times 1$  systems [20]. We therefore assume  $e \neq 0$ . Using the invariance property (i) to divide  $W$  by  $e$ , we have

$$\begin{aligned} W &= \frac{m}{6}\bar{\sigma}^3 + \frac{1}{2}\bar{\sigma}^2\bar{\tau} + \frac{1-k}{6}\bar{\tau}^3, \\ m &= \frac{g}{e}, \quad k = 1 - \frac{b}{e}. \end{aligned} \tag{6.2}$$

This is identical to (5.6).

Equation (4.3) is a special case of (6.2) when  $m = 0$  and the role of  $\bar{\sigma}$  and  $\bar{\tau}$  are interchanged.

## 7. CLASSIFICATION OF GENERAL $2 \times 2$ SYSTEMS NEAR AN UMBILIC POINT

We now study the classification of general  $2 \times 2$  systems in which the potential function  $W$  near an umbilic point is given by (6.2). For simplicity, we omit the overbars and write

$$W(\sigma, \tau) = \frac{m}{3}\sigma^3 + \frac{1}{2}\sigma^2\tau + \frac{1-k}{6}\tau^3. \tag{7.1}$$

The umbilic point is now at the origin. If we change the sign of  $m$  and  $\sigma$ ,  $W$  remains the same. It suffices therefore to consider

$$m > 0,$$

because the wave curves for  $m < 0$  can be obtained from that for  $m > 0$  by reversing the direction of the  $\sigma$ -axis. The wave speeds  $c_1, c_3$  given by (3.2) are

$$\left. \begin{aligned} \eta_1 &= \frac{1}{2} \{2m\sigma + (2-k)\tau - Y\} = (\rho c_1^2)^{-1}, \\ \eta_3 &= \frac{1}{2} \{2m\sigma + (2-k)\tau + Y\} = (\rho c_3^2)^{-1}, \\ Y &= \{(2m\sigma + k\tau)^3 + 4\sigma^2\}^{1/2}. \end{aligned} \right\} \quad (7.2)$$

There is a constant missing in (7.2) due to the omission of the term  $(\sigma^2 + \tau^2)$  in (7.1). Also, (7.2) do not provide the actual wave speeds since  $W$  of (7.1) has been divided by a constant. These do not affect the analyses which follow because we will be concerned with the relative wave speeds, not the absolute wave speeds. The eigenvector  $\mathbf{r} = (r_1, r_2)$  which satisfies the eigenrelation

$$(\mathbf{G} - \eta \mathbf{I})\mathbf{r} = \mathbf{0} \quad (7.3)$$

is tangential to the wave curve and hence, by (3.3),

$$\frac{r_2}{r_1} = \frac{d\tau}{d\sigma} = \frac{2\sigma}{(2m\sigma + k\tau) \mp Y} = \frac{-(2m\sigma + k\tau) \mp Y}{2\sigma}. \quad (7.4)$$

The upper sign is for the  $c_1$  wave curves and the lower sign for the  $c_3$  wave curves. The right hand sides of the equation are homogeneous in  $\sigma$  and  $\tau$  which implies that wave curves are similar. As stated earlier, the wave curves for  $c_1$  and  $c_3$  are orthogonal to each other. Unless stated otherwise, all discussions in the sequel are for the  $c_1$  wave curves. The results of course apply to the  $c_3$  wave curves with minor modifications if necessary.

Equations (7.4) can be integrated in a closed form [21]. It gives a family of wave curves in the  $(\sigma, \tau)$  space. There are straight lines passing through the origin which are themselves wave curves. We call the straight lines wave curves the "wave line". They are determined by seeking the solution of

$$\frac{\tau}{\sigma} = \frac{d\tau}{d\sigma}.$$

The wave lines are then given by

$$\frac{\sigma}{\tau} = 0,$$

and

$$\frac{\sigma}{\tau} = m \pm \sqrt{m^2 + 1 + k}. \quad (7.5)$$

We see that depending on whether  $k$  is less than, equal or larger than  $-(m^2 + 1)$  there will be one, two or three wave lines (Fig. 1). There is an exception for  $k = -1$  at which we have only two wave lines.

Along the wave curve, i.e., along the direction of the eigenvector  $\mathbf{r}$ , the wave speed  $c$  may be increasing or decreasing. If  $\dot{\eta}$  denotes the differentiation of  $\eta$  in the direction of  $\mathbf{r}$ , we have

$$\dot{\eta} = (\nabla \eta) \cdot \mathbf{r}.$$

From (7.2) we see that

$$\begin{aligned} \dot{\eta} &> 0, & \text{if } c \text{ decreases,} \\ \dot{\eta} &< 0, & \text{if } c \text{ increases.} \end{aligned}$$

Differentiation of the eigenrelation (7.3) gives us

$$(\dot{G}_{ij} - \dot{\eta} \delta_{ij})r_i + (G_{ij} - \eta \delta_{ij})\dot{r}_i = 0,$$

and hence

$$r_k r_k \dot{\eta} = \dot{G}_{ii} r_i r_i. \quad (7.6)$$

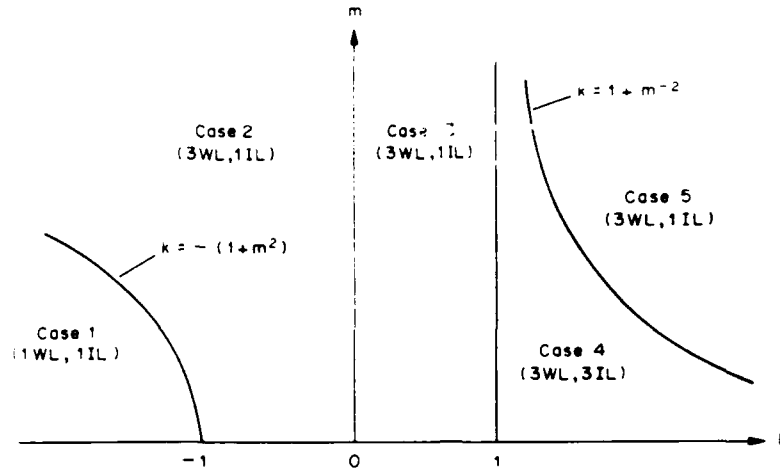


Fig. 1. Classification according to the number of wave lines (WL) and inflection lines (IL).

If we let

$$\sigma = \sigma_1, \quad \tau = \sigma_2,$$

in (7.1), the potential function  $W$  is homogeneous in  $\sigma_1, \sigma_2$  of degree three and has the property

$$\frac{\partial^3 W(\sigma_1, \sigma_2)}{\partial \sigma_i \partial \sigma_j \partial \sigma_k} r_i r_j r_k = 6W(r_1, r_2). \quad (7.7)$$

Noticing that

$$G_{ij} = \frac{\partial^2 W(\sigma_1, \sigma_2)}{\partial \sigma_i \partial \sigma_j},$$

$$\dot{G}_{ij} = \frac{\partial^3 W(\sigma_1, \sigma_2)}{\partial \sigma_i \partial \sigma_j \partial \sigma_k} r_k, \quad (7.8)$$

we obtain from (7.6), (7.8) and (7.7) that

$$\dot{\eta} = \frac{6W(r_1, r_2)}{r_k r_k}. \quad (7.9)$$

Thus the sign of  $\dot{\eta}$  is determined by the sign of  $W(r_1, r_2)$  [11]. In particular, the "inflection" point on the wave curve at which  $\dot{\eta} = 0$  is determined by

$$W(r_1, r_2) = 0. \quad (7.10)$$

Since the wave curves are similar, the inflection points on the wave curves form a straight line passing through the origin which is called the "inflection line". Equation (7.10) is a third order polynomial in  $r_2/r_1$  which means that there exists at least one inflection line.

We now investigate the number of inflection lines. Using (7.1) and (7.4)<sub>1</sub>, we write (7.10) as

$$(1 - k)\Lambda^3 + 3\Lambda + 2m = 0, \quad (7.11)$$

$$\Lambda = \frac{d\tau}{d\sigma}.$$

If  $k = 1$ , we have  $\Lambda = -2m/3$  and  $\Lambda = \infty$ , the latter is a double root. If  $k \neq 1$ , we let

$$\Delta = \left(\frac{m}{1-k}\right)^2 + \left(\frac{1}{1-k}\right)^3. \quad (7.12)$$

We then have one, two or three inflection lines if  $\Delta$  is positive, zero or negative, respectively.

To have three inflection lines we must have

$$m^2 + \frac{1}{1-k} < 0,$$

or

$$1 < k < 1 + m^{-2}.$$

From the above discussion we classify the geometry of wave curves into five cases according to the number of wave lines (WL) and inflection lines (IL) (Fig. 1).

- Case 1:  $k < -(1 + m^2)$ .
- Case 2:  $-(1 + m^2) \leq k \leq 0$ .
- Case 3:  $0 < k \leq 1$ .
- Case 4:  $1 < k < 1 + m^{-2}$ .
- Case 5:  $1 + m^{-2} \leq k$ .

Case 2 and Case 3 have the same number of wave lines and inflection lines but they have quite different wave curve geometry. The special situation in which  $m = 0$  has been studied in [8,9] where Case 5 does not exist. The classification given by Schaeffer and Shearer [11] is based on the potential function

$$W(\sigma, \tau) = \frac{a}{3} \sigma^3 + b\sigma^2\tau + \sigma\tau^2,$$

in which  $a$  and  $b$  are the parameters. This is different from the  $W$  in (7.1) but can be shown to be equivalent if we apply the invariance property (ii). In the  $(a, b)$  plane, Schaeffer and Shearer classify the wave curves into four regions. It can be shown that Case 1, 2, 3, 4 here corresponds, respectively, to Region 4, 3, 2, 1, in [11]. Case 5 here also belongs to Region 2. The boundaries which separate the five cases presented here appear to have a simpler algebraic expression.

Before we investigate in detail each case, we list below some general properties of the wave curves which apply to at least two or more of the five cases. At the point where the wave curve intersects the  $\sigma$ -axis, the slope of the wave curve is obtained from (7.4) as (Fig. 2)

$$\begin{aligned} \frac{d\tau}{d\sigma} &= -(\sqrt{1+m^2} + m), \quad \text{at } \sigma > 0, \quad \tau = 0, \\ &= (\sqrt{1+m^2} - m), \quad \text{at } \sigma < 0, \quad \tau = 0. \end{aligned}$$

This is independent of  $k$  and therefore applies to all five cases. We remind the readers that all

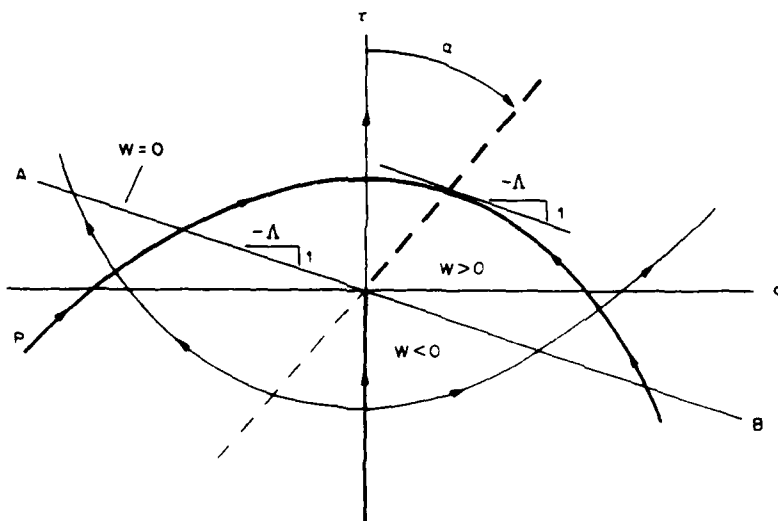


Fig. 2. The wave curves, wave line and inflection line for Case 1.

discussions are for the  $c_1$  wave curves which are represented by bold curves in the figures. We see that the absolute value of the slope at  $\sigma > 0$  is larger than that at  $\sigma < 0$ . Moreover, the product of the two slopes is  $-1$ , which means that the two slopes are orthogonal to each other. Next, the wave lines given by (7.5) apply to  $k \geq - (1 + m^2)$ , i.e. to all cases except Case 1. Let  $\theta_1$  and  $\theta_2$  be the angles the wave lines make with the  $\tau$ -axis. We have

$$\left. \begin{aligned} \tan \theta_1 &= \sqrt{m^2 + 1 + k + m} > 0, & \text{for all } k, \\ \tan \theta_2 &= \sqrt{m^2 + 1 + k - m} \geq 0, & \text{for } k \geq -1. \end{aligned} \right\} \quad (7.13)$$

It is readily shown that  $\theta_1 + \theta_2 < \pi/2$  or  $> \pi/2$  if  $k < 0$  or  $> 0$ . Also,  $\theta_1 > \pi/4$  except when  $-k > 2m < 2$  and  $\theta_2 > \pi/4$  or  $< \pi/4$  when  $k > 2m$  or  $< 2m$ . Finally, for all cases except Case 4, there is only one inflection line. The slope  $\Lambda$  of the wave curve at the point where the wave curve intersects the inflection line is the only real root of (7.11) and is given by

$$\left. \begin{aligned} \Lambda &= \left( \sqrt{\Delta} - \frac{m}{1-k} \right)^{1/3} - \left( \sqrt{\Delta} + \frac{m}{1-k} \right)^{1/3}, \\ \Lambda &\geq 0, \quad \text{if } k \geq 1, \end{aligned} \right\} \quad (7.14)$$

in which  $\Delta$  is defined in (7.12). If we solve (7.4) for  $\tau/\sigma$  in terms of  $d\tau/d\sigma$  (which is  $\Lambda$ ), we obtain

$$\frac{\tau}{\sigma} = \frac{1 - \Lambda^2 - 2m\Lambda}{k\Lambda} = \frac{1 + 2\Lambda^2 + (1 - k)\Lambda^4}{k\Lambda}, \quad (7.15)$$

in which the second equality follows from (7.11). With  $\Lambda$  provided in (7.14), (7.15) furnishes the slope of the only inflection line for Case 1, 2, 3, and 5. We now discuss each case separately.

#### Case 1: $k < -(1 + m^2)$

In Fig. 2, the bold (or thin) lines are the  $c_1$  (or  $c_3$ ) wave curves and the bold (or thin) dotted line is the inflection line for  $c_1$  (or  $c_3$ ). We show in the figure only typical wave curves. Since wave curves are similar, other wave curves can be obtained by enlarging or diminishing the wave curves shown in the figure. The  $\tau$ -axis is a wave line. If  $\alpha$  is the angle the inflection line makes with the positive  $\tau$ -axis, we have from (7.15),

$$\tan \alpha = \frac{k\Lambda}{1 + 2\Lambda^2 + (1 - k)\Lambda^4}, \quad (7.16)$$

where  $\Lambda$  is given in (7.14).  $\Lambda$  is the slope of the wave curve at the intersection of the inflection line. It is also the slope of the line AB on which  $W(\sigma, \tau) = 0$ .

The arrows on the wave curves and the wave line represent the direction along which the wave speed  $c$  decreases, i.e.  $\dot{\eta} > 0$ . This is determined by applying (7.9). For instance, to determine the direction of  $\dot{\eta} > 0$  at point P, we draw from the origin towards the region  $W > 0$  a line parallel to the tangent to the wave curve at P. This determines the direction of the arrow.

#### Case 2: $-(1 + m^2) \leq k \leq 0$

There is one inflection line and (7.16) which gives the angle  $\alpha$  applies here also, Fig. 3. There are three wave lines, one of which is the  $\tau$ -axis while the other two make an angle  $\theta_1$  and  $\theta_2$  with the negative  $\tau$ -axis. Case 2 can be divided into Case 2A and Case 2B depending on whether  $\theta_2 < 0$  or  $> 0$  which is equivalent to  $k < -1$  or  $> -1$ . Each case can be further subdivided according to the relative magnitudes of  $\alpha$ ,  $\theta_1$  and  $\theta_2$ . We have (Fig. 4)

Case 2A<sub>1</sub>:  $0 < \alpha < -\theta_2 = \theta_1$ ,  $(k = -(1 + m^2))$ .

Case 2A<sub>2</sub>:  $0 < \alpha < -\theta_2 < \theta_1$ .

Case 2A<sub>3</sub>:  $0 < -\theta_2 < \alpha < \theta_1$ .

Case 2B<sub>1</sub>:  $0 = \theta_2 < \alpha < \theta_1$ ,  $(k = -1)$ .

Case 2B<sub>2</sub>:  $0 < \theta_2 < \alpha < \theta_1$ .

Case 2B<sub>3</sub>:  $0 < \alpha < \theta_2 < \theta_1$ .

Case 2B<sub>4</sub>:  $0 = \alpha < \theta_2 < \theta_1$ ,  $(k = 0)$ .

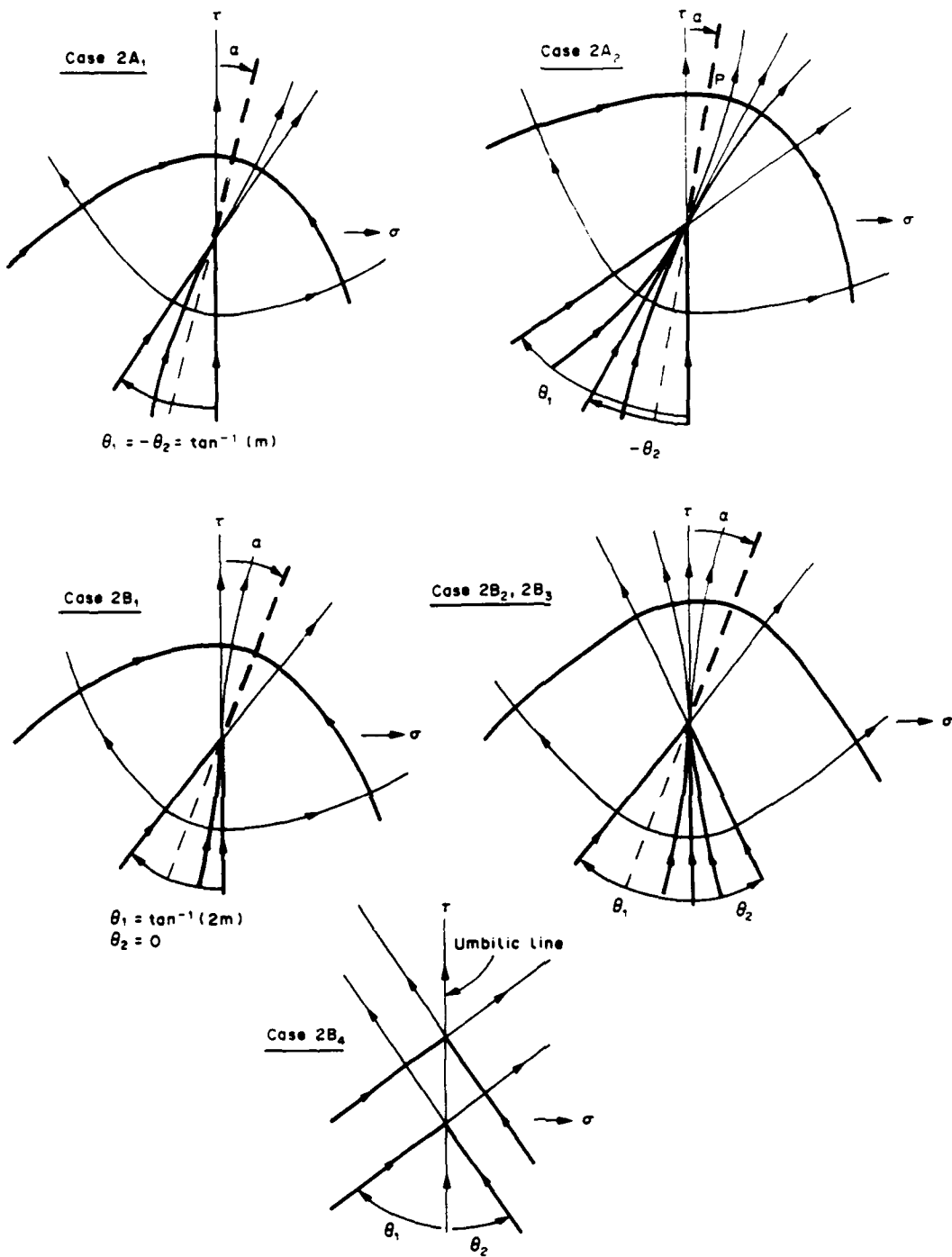


Fig. 3. The wave curves, wave lines and inflection line for Case 2.

In all cases, we have  $\theta_1 < \pi/2$ ,  $\theta_2 < \pi/4$ . The geometry of wave curves, wave lines and the inflection line are shown in Fig. 3. Case 2A<sub>3</sub> is not shown but its geometry is similar to that of Case 2A<sub>2</sub>. Case 2B<sub>4</sub> is a degenerate case in which the  $\tau$ -axis is an umbilic line. It is also a wave line for  $c_1$  as well as for  $c_3$ .

The boundary between Case 2B<sub>2</sub> and Case 2B<sub>3</sub> in Fig. 4 is characterised by the relation

$$\alpha = \theta_2.$$

With  $\alpha$  given by (7.16) and (7.14) and  $\theta_2$  by (7.13)<sub>2</sub>, this boundary can be plotted numerically.

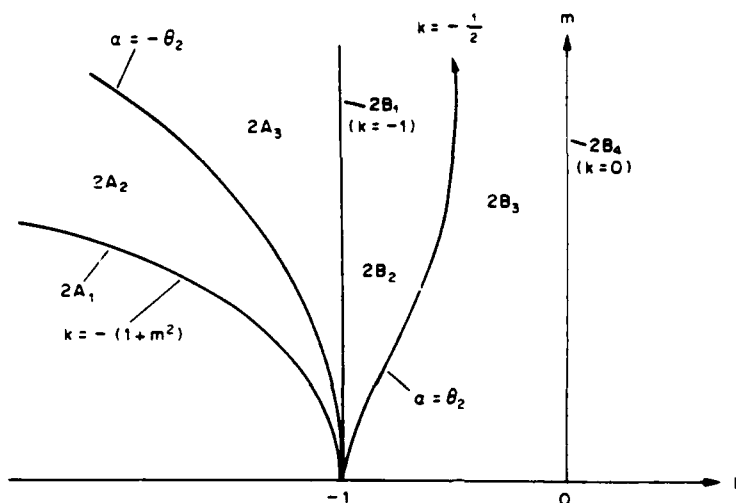


Fig. 4. Further classification of Case 2.

It can be shown that  $k \rightarrow -1/2$  as  $m \rightarrow \infty$ . An alternate way in finding the equation for  $\alpha = \theta_2$  will be given later. [See equation (7.26).] The boundary between Case 2A<sub>2</sub> and 2A<sub>3</sub> is determined by the condition

$$\alpha = -\theta_2.$$

Referring to Case 2A<sub>2</sub> in Fig. 3, this implies that the wave curve and the inflection line are orthogonal to each other at the point of intersection P. With  $\theta_2$  given in (7.13)<sub>2</sub>, the slope  $\Lambda$  of the wave curve at P is

$$\Lambda = \tan \theta_2 = \sqrt{m^2 + 1 + k - m}.$$

Substitution of  $\Lambda$  into (7.11) leads to a fourth order polynomial in  $k$  and  $m$  which can be factorised as

$$[(2+k)^2 + 4m^2][(2-k)^2(k+1) - 4m^2(k-1)] = 0.$$

The first factor is positive and non-zero. We therefore have

$$4m^2 = \frac{k+1}{k-1}(2-k)^2. \quad (7.17)$$

This is the curve denoted by  $\alpha = -\theta_2$  in Fig. 4.

*Case 3:  $0 < k \leq 1$*

Figure 5 shows the geometry of wave curves, wave lines and the only inflection line which makes an angle  $\alpha_0$  with the negative  $\tau$ -axis. The angle  $\alpha_0$  is, from (7.15),

$$\tan \alpha_0 = \frac{-k\Lambda}{1 + 2\Lambda^2 + (1-k)\Lambda^4},$$

and  $\Lambda$  is given in (7.14). It can be shown that

$$0 < \alpha_0 < \theta_2 < \theta_1 < \pi/2.$$

As  $k \rightarrow 0$ ,  $\alpha_0 \rightarrow 0$  and the  $\tau$ -axis becomes an umbilic line. At  $k = 1$ ,

$$\tan \alpha_0 = \frac{6m}{9 + 8m^2}, \quad (7.18)$$

and  $c_1$  on the positive  $\tau$ -axis and  $c_3$  on the negative  $\tau$ -axis assume the same constant value. The  $\tau$ -axis is therefore a shock wave curve.

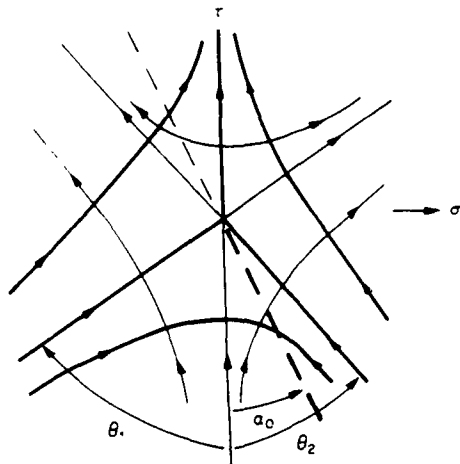


Fig. 5. The wave curves, wave lines and inflection line for Case 3.

**Case 4:  $1 < k < 1 + m^{-2}$** 

This is the most complicated of all five cases. It has three wave lines as well as three inflection lines (Fig. 6). The location of three inflection lines are obtained by the slope  $\Lambda$  of the wave curve at the point of intersection with the inflection line. The slope  $\Lambda$  is a root of (7.11). For Case 4,  $\Delta$  of (7.12) is negative and (7.11) has three real roots. Denoting the three roots by  $\Lambda_0, \Lambda_1, \Lambda_2$ , we have

$$\Lambda_0 = 2(k-1)^{-1/2} \cos\left(\frac{\psi - 2\pi}{3}\right),$$

$$\Lambda_1 = 2(k-1)^{-1/2} \cos\left(\frac{\psi + 2\pi}{3}\right),$$

$$\Lambda_2 = 2(k-1)^{-1/2} \cos\left(\frac{\psi}{3}\right),$$

$$\psi = \cos^{-1}(m\sqrt{k-1}) < \frac{\pi}{2}.$$

The roots are related by the inequalities

$$-\Lambda_0 < -\Lambda_1 < \Lambda_2.$$

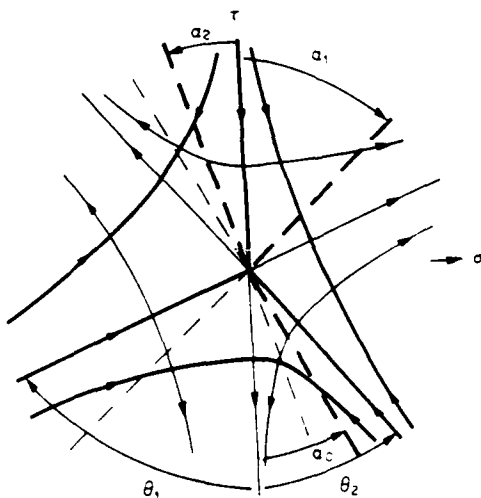


Fig. 6. The wave curves, wave lines and inflection lines for Case 4.

If  $\alpha_0, \alpha_1, \alpha_2$  are the associated angles the inflection lines make with the  $\tau$ -axis, Fig. 6, we obtain from (7.15),

$$\left. \begin{aligned} \tan \alpha_i &= \frac{-k\Lambda_i}{1 + 2\Lambda_i^2 + (1-k)\Lambda_i^4}, & i = 0, 2, \\ \tan \alpha_1 &= \frac{k\Lambda_1}{1 + 2\Lambda_1^2 + (1-k)\Lambda_1^4}. \end{aligned} \right\} \quad (7.19)$$

It can be shown that

$$\left. \begin{aligned} 0 < \alpha_0 < \theta_2 < \theta_1 < \pi/2, \\ 0 < \alpha_2 < \alpha_1, \\ \alpha_1 + \theta_2 < \pi, \quad \alpha_2 + \theta_1 < \pi. \end{aligned} \right\} \quad (7.20)$$

Thus, while  $\alpha_0, \theta_1, \theta_2$  are less than  $\pi/2$ ,  $\alpha_1$  and  $\alpha_2$  can be larger than  $\pi/2$ .

Depending on the relative magnitudes of  $\alpha_0, \alpha_1, \alpha_2, \theta_1$  and  $\theta_2$ , Case 4 can be subdivided as shown in Fig. 7. The subdivisions are obtained by the curves in the  $(k, m)$  plane which represent  $\alpha_1 = \alpha_0, \alpha_1 = \theta_2, \dots$ , etc. Each subregion is identified by one capital letter and one lower case letter. The capital letters represent the following conditions:

- A:  $0 < \alpha_2 < \alpha_0$ .
- B:  $\alpha_0 < \alpha_2 < \theta_2$ .
- C:  $\theta_2 < \alpha_2 < \theta_1$ .
- D:  $\theta_1 < \alpha_2 < \pi/2$ .
- E:  $\pi/2 < \alpha_2 < \pi - \theta_1$ .

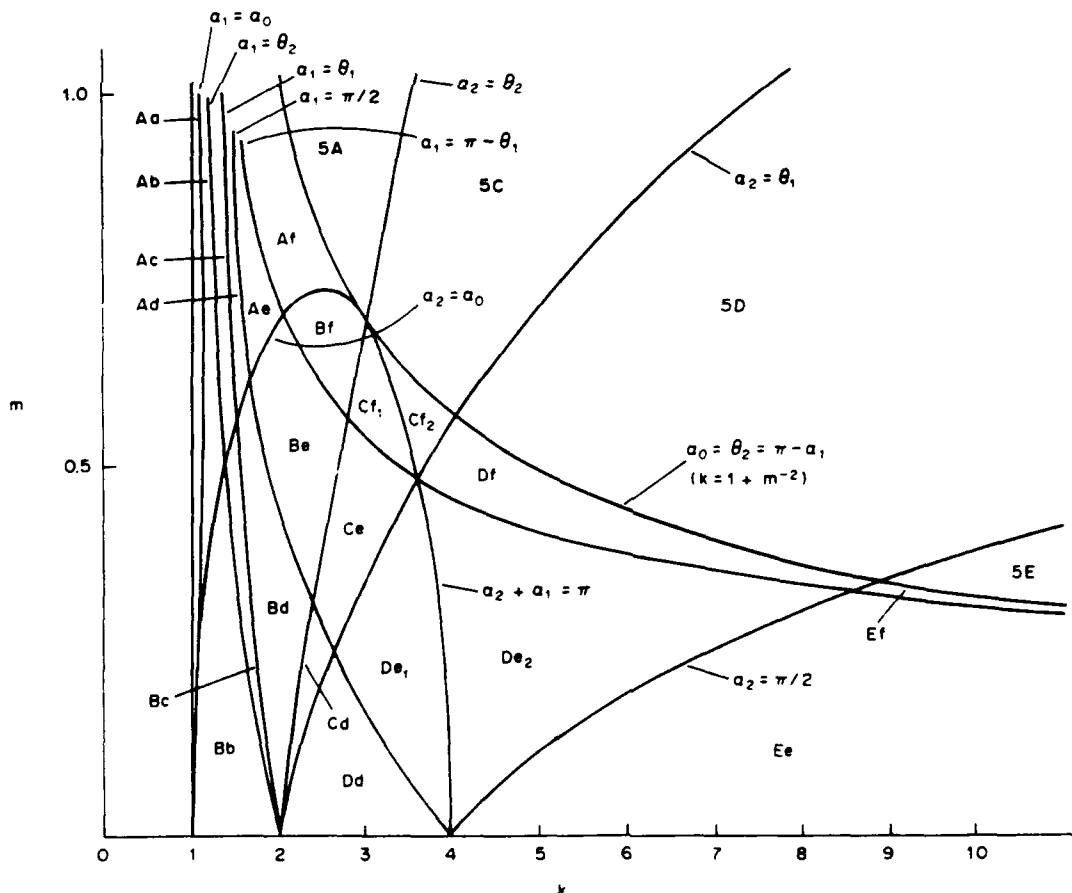


Fig. 7. Further classification of Case 4 and Case 5.

The lower case letters represent the following conditions:

- a:  $0 < \alpha_1 < \alpha_0$ .
- b:  $\alpha_0 < \alpha_1 < \theta_2$ .
- c:  $\theta_2 < \alpha_1 < \theta_1$ .
- d:  $\theta_1 < \alpha_1 < \pi/2$ .
- e:  $\pi/2 < \alpha_1 < \pi - \theta_1$ .
- f:  $\pi - \theta_1 < \alpha_1 < \pi - \theta_2$ .

Therefore, for instance, Case 4Be is governed by the conditions

$$\alpha_0 < \alpha_1 < \theta_2 \quad \text{and} \quad \pi/2 < \alpha_1 < \pi - \theta_1.$$

These conditions are in addition to (7.20) which govern Case 4. Case 4Cf and Case 4De have two more subdivisions. We have

$$\begin{aligned} \alpha_2 &< \pi - \alpha_1 & \text{for Case 4Cf}_1 \text{ and } 4\text{De}_1, \\ \alpha_2 &> \pi - \alpha_1 & \text{for Case 4Cf}_2 \text{ and } 4\text{De}_2. \end{aligned}$$

The equations governing the boundaries between the classifications denoted by  $\alpha_1 = \theta_1$ ,  $\alpha_2 = \alpha_0, \dots$ , in Fig. 7 have the following expressions. They are

$$4m^2 = \frac{k+1}{k-1}(2-k)^2, \quad \text{for } \alpha_1 = \theta_1 \quad \text{or} \quad \alpha_2 = \theta_2, \quad (7.21)$$

$$4m^2 = \frac{(\sqrt{k}-2)^2}{\sqrt{k}-1}, \quad \text{for } \alpha_1 = \pi/2 \quad \text{or} \quad \alpha_2 = \pi/2, \quad (7.22)$$

$$4m^2 = (4-k)(k-1), \quad \text{for } \alpha_2 = \alpha_0 \quad \text{or} \quad \alpha_2 = \pi - \alpha_1, \quad (7.23)$$

$$4m^2 = \frac{(37-30k) \mp (9-2k)\sqrt{9-8k}}{16(k-1)}, \quad \text{for } \alpha_1 = \alpha_0. \quad (7.24)$$

The derivation of (7.21) is similar to that for  $\alpha = -\theta_2$  in Case 2. It is therefore not surprising that (7.21)<sub>1</sub> is identical to (7.17). Equations (7.22)–(7.24) are derived as follows. We substitute  $d\tau/d\sigma$  of (7.4) into (7.11) which results in the following cubic equation for  $\tau/\sigma$ , the slope of the inflection line.

$$a_1 y^3 + a_2 y^2 - a_3 y - a_4 = 0, \quad (7.25)$$

where

$$\begin{aligned} y &= \tau/\sigma, \\ a_1 &= 2mk^3(k-1), \\ a_2 &= 3k^2(k-1)(4m^2 + 1), \\ a_3 &= 6mk[(4-3k) - 4m^2(k-1)], \\ a_4 &= (k-4)^2 + 8m^2(4-3k) - 16m^4(k-1) \\ &= [(\sqrt{k}-2)^2 - 4m^2(\sqrt{k}-1)][(\sqrt{k}+2)^2 + 4m^2(\sqrt{k}+1)]. \end{aligned}$$

If  $\alpha_1 = \pi/2$  or  $\alpha_2 = \pi/2$ ,  $y = 0$  is a root of (7.25). This means that  $a_4 = 0$  which leads to (7.22). If  $\alpha_2 = \alpha_0$ ,  $\alpha_2 = \pi - \alpha_1$ , (7.25) must have a double root for  $y$ . The condition for the cubic equation (7.25) to have a double root can be shown to be given by the equation

$$(k-1)[m^2(k-1)-1][4m^2-(k-1)(4-k)]^2=0.$$

The vanishing of the first factor, i.e.,  $k=1$ , is a degenerate case of Case 4Aa in which  $\alpha_1 = \alpha_2 = 0$ .  $k=1$  is also the boundary between Case 3 and Case 4. The vanishing of the second factor gives the boundary between Case 4 and Case 5 at which  $\alpha_0 = \pi - \alpha_1$ . The vanishing of the third factor leads to (7.23).

When  $\alpha_1 = \alpha_0$ ,  $y = \pm \cot \alpha_0$  are roots of (7.25). This means that (7.25) can be factorized as

$$\begin{aligned} a_1 y^3 + a_2 y^2 - a_3 y - a_4 \\ = (y^2 - \cot^2 \alpha_0)(a_1 y + a_4 \tan^2 \alpha_0), \end{aligned}$$

from which we obtain

$$\tan^2 \alpha_0 = \frac{a_1}{a_3} = \frac{a_2}{a_4}.$$

By a direct substitution, it can be shown that the second equality gives (7.24).

Finally, if we denote the left hand side of (7.25) by  $f(y)$ , we have

$$f(\cot \theta_2) = 0, \quad \text{for } \alpha_1 = \theta_2, \quad (7.26)$$

$$f(-\cot \theta_1) = 0, \quad \text{for } \alpha_1 = \pi - \theta_1 \quad \text{or} \quad \alpha_2 = \theta_1, \quad (7.27)$$

in which  $\theta_1$  and  $\theta_2$  are given in (7.13). It should be pointed out that (7.26) also applies to the curve denoted by  $\alpha = \theta_2$  in Fig. 4 for Case 2.

Two limiting cases of Case 4 are worth mentioned. In the limit  $k = 1$ , we have  $\alpha_1 = \alpha_2 = 0$  and  $\alpha_0$  is given in (7.18). This is a special case of Case 3. At the other limit  $k = 1 + m^{-2}$ , we obtain

$$\alpha_0 = \theta_2 = \pi - \alpha_1 = \tan^{-1}(m^{-1}),$$

$$\tan \alpha_2 = \frac{2(1+m^2)}{m(8m^2-1)}, \quad \tan \theta_1 = 2m + m^{-1}.$$

This belongs to Case 5 which is discussed next.

#### Case 5: $1 + m^{-2} \leq k$

As shown in Fig. 8, there is only one inflection line which makes an angle  $\alpha_2$  with the positive  $\tau$ -axis. From (7.15), we have

$$\tan \alpha_2 = \frac{-k\Lambda}{1 + 2\Lambda^2 + (1-k)\Lambda^4},$$

and  $\Lambda$  is given in (7.14). Case 5 can be subdivided into 5A, 5C, 5D and 5E as shown in Fig. 7.

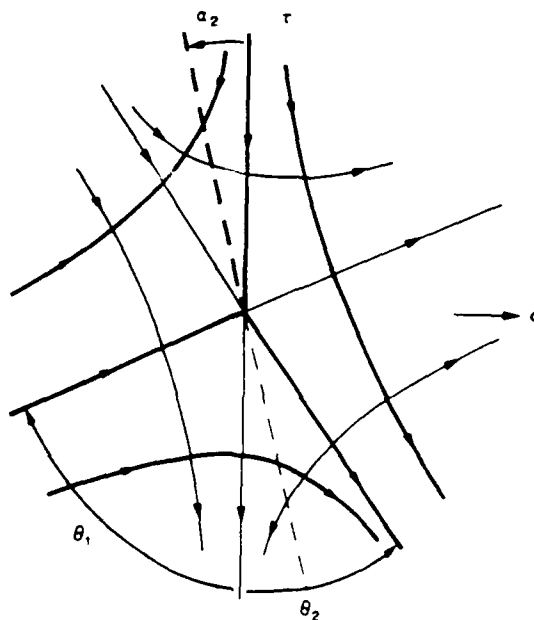


Fig. 8. The wave curves, wave lines and inflection line for Case 5.

The conditions governing the subdivisions are as follows.

- Case 5A:  $0 < \alpha_2 < \theta_2$ .
- Case 5C:  $\theta_2 < \alpha_2 < \theta_1$ .
- Case 5D:  $\theta_1 < \alpha_2 < \pi/2$ .
- Case 5E:  $\pi/2 < \alpha_2 < \pi - \theta_1$ .

Thus  $\alpha_2$  is less than  $\pi/2$  except for Case 5E. The boundaries  $\alpha_2 = \theta_2$ ,  $\alpha_2 = \theta_1$ , and  $\alpha_2 = \pi/2$  between the subdivisions are provided in (7.21), (7.27) and (7.22), respectively.

## 8. CONCLUSIONS

We have presented here a refined classification of  $2 \times 2$  non-strictly hyperbolic systems near an isolated umbilic point for a general potential function. The classification is important in solving the Riemann problem for arbitrarily prescribed constant initial conditions at  $t = 0$ ,  $x > 0$  and constant boundary conditions at  $x = 0$ ,  $t > 0$ .

*Acknowledgement*—The work presented here is supported by the U.S. Air force Office of Scientific Research under Contract AFOSR-89-0013.

## REFERENCES

- [1] P. D. LAX, Hyperbolic systems of conservation laws. II. *Commun. Pure Appl. Math.* **10**, 537–566 (1957).
- [2] C. M. DAFLEROMOS, Quasilinear hyperbolic systems that result from conservation laws. In *Nonlinear Waves* (Edited by S. Leibovich and A. R. Seebase), pp. 82–102. Cornell University Press (1974).
- [3] R. COURANT and D. HILBERT, *Methods of Mathematical Physics*, Vol. II. Interscience, New York (1962).
- [4] A. JEFFREY, *Quasilinear Hyperbolic Systems and Waves*. Pitman (1976).
- [5] J. A. SMOLLER, On the solution of the Riemann problem with general step data for an extended class of hyperbolic systems. *Mich. Math. J.* **16**, 201–210 (1969).
- [6] T.-P. LIU, The Riemann problem for general  $2 \times 2$  conservation laws. *Trans. Am. Math. Soc.* **199**, 89–112 (1974).
- [7] T.-P. LIU, The Riemann problem for general systems of conservation laws. *J. Diff. Eqs* **18**, 218–234 (1975).
- [8] YONGCHI LI and T. C. T. TING, Plane waves in simple elastic solids and discontinuous dependence of solution on boundary conditions. *Int. J. Solids Struct.* **19**, 989–1008 (1983).
- [9] ZHIJING TANG and T. C. T. TING, Wave curves for the Riemann problem of plane waves in isotropic elastic solids. *Int. J. Engng Sci.* **25**, 1343–1381 (1987).
- [10] C. M. DAFLEROMOS, Hyperbolic systems of conservation laws. *Brown University Report*, LCDS 83-5 (1983).
- [11] D. G. SCHAEFFER and M. SHEARER, The classification of  $2 \times 2$  systems of nonstrictly hyperbolic conservation laws, with application to oil recovery. Appendix with D. Marchesin and P. J. Paes-Leme. *Commun. Pure Appl. Math.* **40**, 141–178 (1987).
- [12] J. GLIMM, E. ISAACSON, D. MARCHESIN and O. McBRYAN, Front tracking for hyperbolic systems. *Adv. Appl. Math.* **2**, 91–119 (1981).
- [13] J. GLIMM, C. KLINGENBERG, O. McBRYAN, B. PLOHR, D. SHARP and S. YANIV, Front tracking and two-dimensional Riemann problems. *Adv. Appl. Math.* **6**, 259–290 (1985).
- [14] B. L. KEYFITZ and H. C. Kranzer, A system of hyperbolic conservation laws arising in elasticity theory. *Arch. Rat. Mech. Anal.* **72**, 219–241 (1980).
- [15] B. L. KEYFITZ and H. C. Kranzer, The Riemann problem for a class of conservation laws exhibiting a parabolic degeneracy. *J. Diff. Eqs* **47**, 35–65 (1983).
- [16] E. ISAACSON and J. B. TEMPLE, Examples and classification of non-strictly hyperbolic systems of conservation laws. *Abstr. Papers Presented to AMS* **6**, 60 (1985).
- [17] M. SHEARER, D. G. SCHAEFFER, D. MARCHESIN and P. J. PAES-LEME, Solution of the Riemann problem for a prototype  $2 \times 2$  system of non-strictly hyperbolic conservation laws. *Arch. Rat. Mech. Anal.* **97**, 299–320 (1987).
- [18] D. G. SCHAEFFER and M. SHEARER, Riemann problems for nonstrictly hyperbolic  $2 \times 2$  systems of conservation laws. *Trans. Am. Math. Soc.* **304**, 267–306 (1987).
- [19] C. TRUESDELL and W. NOLL, *The Nonlinear Field Theories of Mechanics. Handbuch der Physik*, Vol III/3. Springer, Berlin (1965).
- [20] T. C. T. TING, The Riemann problem with umbilic lines for wave propagation in isotropic elastic solids. *Notes in Numerical Fluids Mechanics*, Vol. 24: *Nonlinear Hyperbolic Equations—Theory, Numerical Methods and Applications* (Edited by J. Ballmann and R. Jeltsch), pp. 617–629. Vieweg, (1988).
- [21] T. C. T. TING, On wave propagation problems in which  $c_1 = c_2 = c_3$  occurs. *Q. Appl. Math.* **31**, 275–286 (1973).
- [22] GUANGSHAN ZHU and T. C. T. TING, Wave curves with the presence of an umbilic point and an umbilic line for plane waves in isotropic elastic solids. To appear.

(Received 8 March 1989)

---

---

## CHAPTER 15

### Growth or Decay of Shock Waves in the Generalized Goursat-Riemann Problem\*

T. C. T. Ting†  
Tankin Wang†

**Abstract.** For plane waves propagating in an elastic half-space  $x \geq 0$  due to an impact at the plane  $x = 0$ , the problem is that of a generalized Goursat-Riemann problem in which the initial conditions at  $t = 0$  are constant but the boundary conditions at  $x = 0$  are not. If  $\mathbf{s}(x, t)$  is the traction vector at any plane  $x = \text{constant}$ ,  $\mathbf{s}(0, t)$  depends on  $t$ . Assuming that  $\mathbf{s}(0, t)$  is linear in  $t$ , i.e.,  $\mathbf{s}(0, t) = \mathbf{s}^a + \mathbf{s}_t^a t$  where  $\mathbf{s}^a$  and  $\mathbf{s}_t^a$  are constant, the Goursat-Riemann problem corresponds to the special case in which  $\mathbf{s}_t^a$  vanishes. We study the generalized Goursat-Riemann problem with non-zero  $\mathbf{s}_t^a$ . We investigate how the solution to the Goursat-Riemann problem is affected by the non-zero  $\mathbf{s}_t^a$ . In particular, we examine whether the shock waves generated in the Goursat-Riemann problem grow or decay due to the non-zero  $\mathbf{s}_t^a$ .

**1. Introduction.** The equations governing the plane waves in an isotropic elastic solid, with certain restrictions, can be written as a system of  $4 \times 4$  conservation laws [1,2],

$$\mathbf{U}_x - \mathbf{f}(\mathbf{U})_t = \mathbf{0}. \quad (1)$$

$$\mathbf{U} = (\sigma, \tau, u, v),$$

$$\mathbf{f}(\mathbf{U}) = (\rho u, \rho v, \varepsilon, \gamma).$$

---

\*The work presented here is supported by the U. S. Air Force Office of Scientific Research under Contract AFSOR-89-0013

†Department of Civil Engineering, Mechanics and Metallurgy, University of Illinois at Chicago,  
Box 4348, Chicago, IL 60680.

In the above,  $\sigma, \tau$  are the normal and shear stresses,  $\varepsilon, \gamma$  are the normal and shear strains,  $u, v$  are the normal and transverse velocities and  $\rho$  is the mass density. For hyperelastic solids there exists a potential function, or the complementary strain energy  $W(\sigma, \tau)$  such that [3]

$$\varepsilon = W_\sigma, \quad \gamma = W_\tau, \quad (2)$$

in which the subscript denotes differentiation. Introducing the 2-vectors

$$\mathbf{s} = (\sigma, \tau), \quad \mathbf{u} = (u, v), \quad \mathbf{p} = (\varepsilon, \gamma), \quad (3)$$

equation (1) can be written for continuous solutions as

$$\mathbf{U}_t - \mathbf{A}\mathbf{U}_t = \mathbf{0}, \quad \mathbf{U} = \begin{bmatrix} \mathbf{s} \\ \mathbf{u} \end{bmatrix}, \quad (4)$$

$$\mathbf{A} = \begin{bmatrix} \mathbf{0} & \rho\mathbf{I} \\ \mathbf{G} & \mathbf{0} \end{bmatrix},$$

where  $\mathbf{I}$  is a unit matrix and

$$\mathbf{G} = \begin{bmatrix} W_{\sigma\sigma} & W_{\sigma\tau} \\ W_{\sigma\tau} & W_{\tau\tau} \end{bmatrix}. \quad (5)$$

The characteristic wave speed  $c$  is obtained from [4]

$$(c\mathbf{A} + \mathbf{I})\boldsymbol{\xi} = \mathbf{0}, \quad \boldsymbol{\xi} = \begin{bmatrix} \mathbf{r} \\ -\mathbf{r}/(\rho c) \end{bmatrix}, \quad (6)$$

which can be reduced to

$$\{\mathbf{G} - (\rho c^2)^{-1}\mathbf{I}\} \mathbf{r} = \mathbf{0}. \quad (7)$$

Assuming that  $\mathbf{G}$  is positive definite, there are two pairs of characteristic wave speeds  $\pm c_1, \pm c_3$  and we let

$$c_1 \geq c_3 > 0.$$

Had we considered fully general plane waves, (1) would be a system of  $6 \times 6$  conservation laws and there would be an additional pair of characteristic wave speed  $\pm c_2$ , which can be shown to be linearly degenerate [2].

It should be pointed out that (7) is, mathematically, the characteristic equation with characteristic wave speed  $(\rho c^2)^{-1}$  for the following  $2 \times 2$  conservation laws

$$\left. \begin{aligned} s_t + f(s)_x &= 0, \\ s = (\sigma, \tau), \quad f(s) &= (W_\sigma, W_\tau). \end{aligned} \right\} \quad (8)$$

Equation (8) is a familiar equation in fluid dynamics and hence the results obtained here can be applied to problems in fluid dynamics. Many studies have been made on (8) which is in general not strictly hyperbolic [5-9].

In this paper we consider the following initial and boundary conditions for the generalized Goursat-Riemann problem

$$\left. \begin{aligned} s(x, 0) &= s^b, \quad x > 0, \\ s(0, t) &= s^a + s_t^a t, \quad t > 0, \end{aligned} \right\} \quad (9)$$

where  $s^b, s^a, s_t^a$  are constant. The superscripts "b" and "a" stand for "before" and "after", respectively. The constants  $s^b, s^a, s_t^a$  are 2-vectors defined in (3)<sub>1</sub>. The problem reduces to the Goursat-Riemann problem when  $s_t^a = 0$ .

When  $s_t^a = 0$ ,  $U(x, t)$  depends on  $x/t$  only and is best expressed in the form of wave curves in the  $U$  space. The wave curve consists of a sequence of simple wave curves and/or shock wave curves [10]. If the boundary conditions are prescribed in terms of stress  $s$ , it suffices to consider wave curves in the sub-space  $s$  [1.2]. This is not possible if the boundary conditions are prescribed in terms of velocity [11.12]. The simple waves are "centered simple waves" because, in the  $x-t$  plane, they are represented by a family of straight lines from the origin  $x=t=0$ . Along each straight line  $U$  is a constant. The shock wave in the  $x-t$  plane is represented by a double line which is a straight line because the shock wave speed is a constant. Between the simple waves and/or the shock waves we have constant state regions. When  $s_t^a \neq 0$ , we no longer have simple waves and constant state regions. Moreover, the shock wave speed is not a constant and may grow or decay as time increases. We will investigate the perturbation of the solution to the generalized Goursat-Riemann problem from the Goursat-Riemann problem in the region near  $x = 0$  and  $t = 0$ . In particular, we examine whether the shock waves grow or decay due to the non-zero

$s_t^a$ . The perturbation is with respect to small  $x$  and  $t$ , not with  $s_t^a$ , so that the value of  $s_t^a$  need not be small.

**2. Perturbation in the constant state and simple wave regions.** For the generalized Goursat-Riemann problem with initial and boundary conditions prescribed in (9) we consider the solution  $\mathbf{U}(x, t)$  in the form [13-15]

$$\left. \begin{aligned} \mathbf{U}(x, t) &= \mathbf{U}^0(\lambda) + t \mathbf{U}^1(\lambda) + \frac{t^2}{2} \mathbf{U}^2(\lambda) + \dots, \\ \lambda &= x/t, \end{aligned} \right\} \quad (10)$$

where  $\mathbf{U}^0, \mathbf{U}^1, \mathbf{U}^2, \dots$  are functions of  $\lambda$  only. Clearly,  $\mathbf{U}^1, \mathbf{U}^2, \dots$  vanish identically for the Goursat-Riemann problem. Differentiation of (10) with  $x$  and  $t$  results in

$$\left. \begin{aligned} \mathbf{U}_x &= \frac{1}{t} \frac{d}{d\lambda} \mathbf{U}^0 - \frac{d}{d\lambda} \mathbf{U}^1 - O(t), \\ \mathbf{U}_t &= -\frac{\lambda}{t} \frac{d}{d\lambda} \mathbf{U}^0 + (\mathbf{U}^1 - \lambda \frac{d}{d\lambda} \mathbf{U}^1) + O(t). \end{aligned} \right\} \quad (11)$$

Since  $\mathbf{A}$  in (4) depends on  $\mathbf{U}$ , we also expand  $\mathbf{A}$  as

$$\mathbf{A}(\mathbf{U}) = \mathbf{A}^0(\lambda) + t \mathbf{A}^1(\lambda) + \frac{t^2}{2} \mathbf{A}^2(\lambda) + \dots \quad (12)$$

$$\left. \begin{aligned} \mathbf{A}^0(\lambda) &= \mathbf{A}(\mathbf{U}^0) \\ \mathbf{A}^1(\lambda) &= \mathbf{U}^1 \cdot \nabla \mathbf{A}^0 \\ &\vdots \end{aligned} \right\} \quad (13)$$

The operator  $\nabla$  is the gradient with respect to the components of  $\mathbf{U}$ . With (11) and (12), (4)<sub>1</sub> leads to

$$(\lambda \mathbf{A}^0 + \mathbf{I}) \frac{d}{d\lambda} \mathbf{U}^0 = \mathbf{0}, \quad (14)$$

$$(\lambda \mathbf{A}^0 + \mathbf{I}) \frac{d}{d\lambda} \mathbf{U}^1 = \mathbf{A}^0 \mathbf{U}^1 - \lambda \mathbf{A}^1 \frac{d}{d\lambda} \mathbf{U}^0. \quad (15)$$

We will study the first order perturbation, namely, the solution of  $\mathbf{U}^1$ .

Let  $c^0$  be a root of the determinant

$$\|c^0 \mathbf{A}^0(c^0) + \mathbf{I}\| = 0.$$

The solution of  $\mathbf{U}^0, \mathbf{U}^1$  depends on whether  $\lambda$  equals to any of the four roots  $c^0$  or not. We call the region "regular" if  $\lambda \neq c^0$  and "singular" if  $\lambda = c^0$ . For the Goursat-Riemann problem the regions  $\lambda \neq c^0$  and  $\lambda = c^0$  correspond, respectively, to the constant state region and the simple wave region.

**2.1 Regular region.** When  $\lambda \neq c^0$ , (14) and (15) yield

$$\left. \begin{array}{l} \mathbf{U}^0 = \text{constant}, \\ \mathbf{U}^1 = \{(\mathbf{A}^0)^{-1} + \lambda \mathbf{I}\} \mathbf{q}, \end{array} \right\} \quad (16)$$

where  $\mathbf{q}$  is an arbitrary constant. Equation (11)<sub>2</sub> then gives

$$\mathbf{U}_{t=0} = (\mathbf{A}^0)^{-1} \mathbf{q}, \quad (17)$$

and (16) and (17) provide the relation

$$\mathbf{U}^1 = (\lambda \mathbf{A}^0 + \mathbf{I}) \mathbf{U}_{t=0} \quad (18)$$

which allows us to convert  $\mathbf{U}_{t=0}$  to  $\mathbf{U}^1$  and vice versa. We see that while  $\mathbf{U}^0, \mathbf{U}_{t=0}$  are constant,  $\mathbf{U}^1$  is linear in  $\lambda$ .

**2.2 Singular region.** When

$$\lambda = c^0, \quad (19)$$

equations (14) and (6)<sub>1</sub> imply that

$$\frac{d}{d\lambda} \mathbf{U}^0 = -\zeta \boldsymbol{\xi}^0$$

where  $\zeta$  is a proportionality factor. In particular,

$$\frac{d}{d\lambda} \mathbf{s}^0 = -\zeta \mathbf{r}^0. \quad (20)$$

The proportionality factor  $\zeta$  is determined by differentiating (19) with  $\lambda$  and using (20). We have

$$1 = -\zeta \mathbf{r}^0 \cdot \nabla c^0 \quad (21)$$

and (20) is rewritten as

$$\frac{d}{d\lambda} \mathbf{s}^0 = \{\mathbf{r}^0 \cdot \nabla c^0\}^{-1} \mathbf{r}^0. \quad (22)$$

It is clear that  $\nabla$  here is the gradient with respect to the components of  $\mathbf{s}$  because  $c$  depends on  $\mathbf{s}$ , not on  $\mathbf{u}$ . Integration of (20) or (22) furnishes the simple wave curves in the stress space [1,2].

Inserting (13)<sub>2</sub> in (15) we obtain the differential equation for  $\mathbf{U}^1$  for the singular region as

$$(\lambda \mathbf{A}^0 + \mathbf{I}) \frac{d}{d\lambda} \mathbf{U}^1 = \mathbf{A}^0 \mathbf{U}^1 - \lambda \mathbf{U}^1 \cdot (\nabla \mathbf{A}^0) \frac{d}{d\lambda} \mathbf{U}^0 \quad (23)$$

which is linear in  $\mathbf{U}^1$ . Hence if  $\mathbf{U}^1$  is a solution, so is  $k\mathbf{U}^1$  where  $k$  is an arbitrary constant. Despite the fact that the coefficient of  $d\mathbf{U}^1/d\lambda$  in (23) is singular, it is shown in [13] that (23) can be solved for  $d\mathbf{U}^1/d\lambda$  and that the solution for  $\mathbf{U}^1$  is unique.

**3. Discontinuity of  $\mathbf{U}^1$  between the singular and regular regions.**  
We consider  $\mathbf{U}(x,t)$  on a curve  $\Gamma$  in the  $x-t$  plane which is given by

$$x_\Gamma = \lambda_\Gamma t + \frac{1}{2} \kappa_\Gamma t^2 + \dots$$

where  $\lambda_\Gamma$  and  $\kappa_\Gamma$  are constant. The curvature of  $x_\Gamma$  at  $t = 0$  is  $\kappa_\Gamma$ . Hence

$$\lambda = x_\Gamma/t = \lambda_\Gamma + \frac{1}{2} \kappa_\Gamma t + \dots$$

and, from (10),  $\mathbf{U}(x,t)$  on  $\Gamma$  is

$$\mathbf{U}(x_\Gamma, t) = \mathbf{U}^0(\lambda_\Gamma) + t \left\{ \mathbf{U}^1 + \frac{1}{2} \kappa_\Gamma \frac{d}{d\lambda} \mathbf{U}^0 \right\} \Big|_{\lambda=\lambda_\Gamma} + O(t^2).$$

If  $\Gamma$  is a boundary between a regular region and a singular region and if  $\Gamma$  is not a shock wave,  $\mathbf{U}(x,t)$  and  $\mathbf{U}^0(\lambda_\Gamma)$  are continuous across  $\Gamma$ . We then have

$$\{U^1\}_{\text{regular region}} = \{U^1 + \frac{1}{2} \kappa_r \frac{d}{d\lambda} U^0\}_{\text{singular region}} \quad (24)$$

This shows that  $U^1$  is in general discontinuous across the boundary between a regular region and a singular region even when  $U(x, t)$  is continuous.

**4. Perturbation of the shock wave solution.** The Rankine-Hugoniot equation for (1) is

$$[U] + V^* [f(U)] = 0 \quad (25)$$

in which  $V^*$  is the shock wave speed and the square brackets denote the jump across the shock wave. Employing the 2-vectors (3), (25) can be written as

$$\left. \begin{aligned} [\mathbf{s}] + \rho V^* [\mathbf{u}] &= \mathbf{0} \\ [\mathbf{u}] - V^* [\mathbf{p}] &= \mathbf{0} \end{aligned} \right\} \quad (26)$$

Let  $x_v(t)$  be the locus of the shock wave in the  $x-t$  plane and be given by

$$x_v = Vt + \frac{1}{2} \kappa_v t^2 + \dots$$

where  $V, \kappa_v$  are respectively, the initial velocity and the initial acceleration of the shock wave at  $t = 0$ . The shock wave speed  $V^*$  at anytime  $t$  is

$$V^* = V + \kappa_v t + \dots \quad (27)$$

Equation (10) written for  $\mathbf{u}$  and  $\mathbf{s}$  are

$$\left. \begin{aligned} \mathbf{u}(x, t) &= \mathbf{u}^0 + t \mathbf{u}^1 + \frac{t^2}{2} \mathbf{u}^2 + \dots \\ \mathbf{s}(x, t) &= \mathbf{s}^0 + t \mathbf{s}^1 + \frac{t^2}{2} \mathbf{s}^2 + \dots \end{aligned} \right\} \quad (28)$$

With the notations (3)<sub>3</sub>, (2) can be written as

$$p_i = \frac{\partial W}{\partial s_i}$$

and the expression of  $\mathbf{p}$  in the form (10) leads to

$$\begin{aligned}\mathbf{p}(\mathbf{s}) &= \mathbf{p}^0 + t \mathbf{p}^1 + \frac{t^2}{2} \mathbf{p}^2 + \dots, \\ \mathbf{p}^0 &= \mathbf{p}(\mathbf{s}^0), \quad \mathbf{p}^1 = \mathbf{G}^0 \mathbf{s}^1, \\ p_i^2 &= G_{ij}^0 s_j^2 - \frac{\partial^3 V}{\partial s_i \partial s_j \partial s_k} s_j^1 s_k^1.\end{aligned}\tag{29}$$

In the above,  $\mathbf{G}^0 = \mathbf{G}(\mathbf{s}^0)$ . Substituting (27)-(29) into (26), we have

$$\left. \begin{aligned} [\mathbf{s}^0] - \rho V [\mathbf{u}^0] &= \mathbf{0} \\ [\mathbf{u}^0] - V [\mathbf{p}^0] &= \mathbf{0} \end{aligned} \right\} \tag{30}$$

for the zero order and

$$\left. \begin{aligned} [\mathbf{s}^1] + \rho V [\mathbf{u}^1] - \rho \kappa_v [\mathbf{u}^0] &= \mathbf{0} \\ [\mathbf{u}^1] + V [\mathbf{G}^0 \mathbf{s}^1] + \kappa_v [\mathbf{p}^0] &= \mathbf{0} \end{aligned} \right\} \tag{31}$$

for the first order.

From (30) we obtain

$$[\mathbf{u}^0] = -\frac{1}{\rho V} [\mathbf{s}^0], \quad [\mathbf{p}^0] = \frac{1}{\rho V^2} [\mathbf{s}^0], \tag{32}$$

and the use of these results in (31) leads to

$$\left. \begin{aligned} \rho V [\mathbf{u}^1] &= -[\mathbf{s}^1] - (\kappa_v/V) [\mathbf{s}^0], \\ [\mathbf{u}^1] &= -V [\mathbf{G}^0 \mathbf{s}^1] - (\kappa_v/\rho V^2) [\mathbf{s}^0]. \end{aligned} \right\} \tag{33}$$

Elimination of  $[\mathbf{u}^1]$  between the two equations in (33) yields

$$\rho V^2 [\mathbf{G}^0 \mathbf{s}^1] - [\mathbf{s}^1] = -2(\kappa_v/V) [\mathbf{s}^0]. \tag{34}$$

Let  $s^+, s^-$  be respectively the value of  $s$  in front of and behind the shock wave. When  $s^+$  is given, (32) provides a solution for  $s^-$  with  $V$  as the parameter.

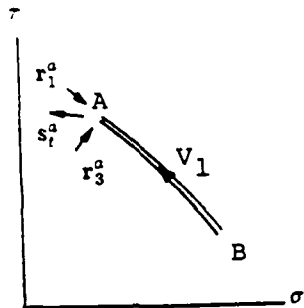


Fig.1 The shock wave curve in the stress space

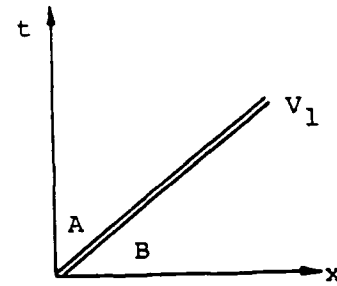


Fig.2 The solution for the Goursat-Riemann problem when  $s_t^a = 0$

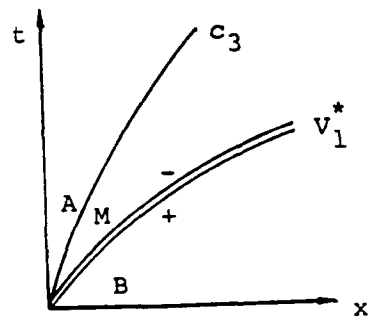


Fig.3 The solution for the generalized Goursat-Riemann problem with  $s_t^a \neq 0$

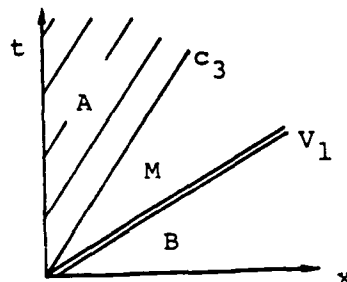


Fig.4 The solution to the special case when  $s_t^a = r_3^a r_3^a$

As  $V$  varies,  $\mathbf{s}^-$  traces out a curve in the stress space which is the shock wave curve. Fig. 1. Equation (32)<sub>1</sub> then gives the jump in  $\mathbf{u}^0$  while (34) and (33)<sub>1</sub> or (33)<sub>2</sub> give the jump in  $\mathbf{s}^1$  and  $\mathbf{u}^1$  in terms of  $\kappa_v$ .

**5. Growth or decay of the shock wave.** When the initial acceleration  $\kappa_v$  of the shock wave is non-zero, the shock wave grows or decays as it propagates. If the state ahead of the shock wave is at rest or at a uniform state, the stress amplitude and velocity amplitude in general increase or decrease according to whether the acceleration  $\kappa_v$  is positive or negative. If the state ahead of the shock wave is not a uniform state, the positivity of  $\kappa_v$  may not be accompanied by the growth of the stress amplitude and/or the velocity amplitude. This was pointed out in [16] for one-dimensional shock waves and in [17-19] for three-dimensional shock waves. Thus the definition of growth or decay of a shock wave depends on whether one is looking at the stress amplitude, the velocity amplitude or the acceleration  $\kappa_v$ .

In this paper we define the growth or decay of shock waves according to whether  $\kappa_v$  is positive or negative.

**6. The solution to the generalized Goursat-Riemann problem.** The perturbation  $\mathbf{U}^1$  presented in Sections 2, 4 and the discontinuity condition of  $\mathbf{U}^1$  between the singular and regular regions derived in Section 3 are the basis for the constructing the solution  $\mathbf{U}^1$  to the generalized Goursat-Riemann problem prescribed in (9). As an illustration, consider the special case in which  $\mathbf{s}^a, \mathbf{s}^b$  in (9) are located on a shock wave curve associated with  $c_1$  which is denoted by  $V_1$  in Fig. 1. If  $s_t^a = 0$ , the solution in the  $x-t$  plane consists of a single shock wave of wave speed  $V_1$ , Fig. 2. Since  $\mathbf{s}_t^a \neq \mathbf{0}$ , we would have the wave pattern shown in Fig. 3 in which there is a non-constant shock wave  $V_1^*$  followed by an acceleration wave  $c_3$ . The acceleration wave  $c_1$  does not appear because, by Lax stability conditions [20], the  $c_1$  wave speed behind the shock wave is larger than the shock wave speed  $V_1^*$ . The region between the  $V_1^*$  shock wave and the  $c_3$  acceleration wave denoted by M is a regular region which is not a constant state. We will determinate the initial acceleration  $\kappa_v$  of the  $V_1^*$  shock and  $s_t^m$  which is the value of  $s_t$  in the region M as  $t \rightarrow 0$ . In the sequel, the superscripts  $a, b, m, \dots$  denote the value of the quantity concerned in the regions  $A, B, M, \dots$ , respectively, as  $t \rightarrow 0$ .

The first step is to find  $\mathbf{U}^{1+}$  from  $\mathbf{U}^{1-}$  across the shock wave  $V_1^*$ . Applying (34) to the shock wave  $V_1^*$  at  $t = 0$  and noticing that the region B is a constant state which means that  $\mathbf{U}^{1+} = \mathbf{0}$ , we have

$$\rho V_1^2 \mathbf{G}^a \mathbf{s}^{1-} - \mathbf{s}^{1-} = -2(\kappa_v V_1) \mathbf{s}^0. \quad (35)$$

The regions M and A are both regular regions and hence  $s^a = s^m$  which leads to  $\mathbf{G}^a = \mathbf{G}^m$ . Let

$$\mathbf{s}^{1-} = \gamma_1^- \mathbf{r}_1^a + \gamma_3^- \mathbf{r}_3^a, \quad (36)$$

$$[\mathbf{s}^0] = \mathbf{s}^a - \mathbf{s}^b = -(\gamma_1^0 \mathbf{r}_1^a + \gamma_3^0 \mathbf{r}_3^a), \quad (37)$$

in which  $\gamma_1^-, \gamma_3^-, \gamma_1^0, \gamma_3^0$  are constant and  $\mathbf{r}_1^a, \mathbf{r}_3^a$  are the right eigenvectors of (7) associated with  $c = c_1^a, c_3^a$ , i.e.,

$$\left. \begin{array}{l} \{\rho(c_1^a)^2 \mathbf{G}^a - \mathbf{I}\} \mathbf{r}_1^a = \mathbf{0}, \\ \{\rho(c_3^a)^2 \mathbf{G}^a - \mathbf{I}\} \mathbf{r}_3^a = \mathbf{0}. \end{array} \right\} \quad (38)$$

In the above it is understood that  $c_1^- = c_1^a$  and  $c_3^- = c_3^a$ . The direction of  $\mathbf{r}_1^a$  and  $\mathbf{r}_3^a$  are taken to be in the direction of decreasing  $c_1$  and  $c_3$ , respectively. With  $[\mathbf{s}^0]$  given in (9),  $\gamma_1^0$  and  $\gamma_3^0$  are determined from (37). For the  $V_1$  shock wave and the  $\mathbf{r}_1^a, \mathbf{r}_3^a$  shown in Fig. 1, we have

$$\gamma_1^0 > 0. \quad (39)$$

Using (36)-(38), (35) can be written as

$$\begin{aligned} & \{(V_1/c_1^a)^2 - 1\} \gamma_1^- \mathbf{r}_1^a + \{(V_1/c_3^a)^2 - 1\} \gamma_3^- \mathbf{r}_3^a \\ &= 2(\kappa_v/V_1)(\gamma_1^0 \mathbf{r}_1^a + \gamma_3^0 \mathbf{r}_3^a). \end{aligned}$$

Hence  $\gamma_1^-$  and  $\gamma_3^-$  are given by

$$\left. \begin{array}{l} \{(V_1/c_1^a)^2 - 1\} \gamma_1^- = 2(\kappa_v/V_1) \gamma_1^0 \\ \{(V_1/c_3^a)^2 - 1\} \gamma_3^- = 2(\kappa_v/V_3) \gamma_3^0 \end{array} \right\} \quad (40)$$

with  $\kappa_v$  as an unknown parameter. We have thus obtained  $\mathbf{s}^{1-}$  of (36). As to  $\mathbf{u}^{1-}$ , using (36) and (37), we write (33)<sub>1</sub> as

$$\rho V_1 \mathbf{u}^{1-} = -(\gamma_1^- \mathbf{r}_1^a + \gamma_3^- \mathbf{r}_3^a) - (\kappa_v/V_1)(\gamma_1^0 \mathbf{r}_1^a + \gamma_3^0 \mathbf{r}_3^a).$$

We are interested in  $\rho V_1 \mathbf{u}^{1-} - \mathbf{s}^{1-}$ , not in  $\rho V_1 \mathbf{u}^{1+}$ . Therefore we employ (36) and (40) to obtain

$$\rho V_1 \mathbf{u}^{1-} - \mathbf{s}^{1-} = -\frac{(V_1/c_1^a)^2 + 3}{(V_1/c_1^a)^2 - 1} \left( \frac{\kappa_r}{V_1} \right) \gamma_1^0 \mathbf{r}_1^a - \frac{(V_1/c_3^a)^2 + 3}{(V_1/c_3^a)^2 - 1} \left( \frac{\kappa_r}{V_1} \right) \gamma_3^0 \mathbf{r}_3^a. \quad (41)$$

The next step is to convert  $\mathbf{U}^{1-}$  to  $\mathbf{U}_t^m$  using (18) which is written in full as

$$\mathbf{s}^{1-} = \mathbf{s}_t^m + \rho V_1 \mathbf{u}_t^m,$$

$$\mathbf{u}^{1-} = V_1 \mathbf{G}^a \mathbf{s}_t^m + \mathbf{u}_t^m.$$

Eliminating  $\mathbf{u}_t^m$  leads to

$$\rho V_1 \mathbf{u}^{1-} - \mathbf{s}^{1-} = (\rho V_1^2 \mathbf{G}^a - \mathbf{I}) \mathbf{s}_t^m. \quad (42)$$

To determine  $\mathbf{s}_t^m$  explicitly, we let

$$\mathbf{s}_t^m = \gamma_1^m \mathbf{r}_1^a + \gamma_3^m \mathbf{r}_3^a, \quad \mathbf{s}_t^a = \gamma_1^a \mathbf{r}_1^a + \gamma_3^a \mathbf{r}_3^a, \quad (43)$$

where  $\gamma_1^m, \gamma_3^m, \gamma_1^a, \gamma_3^a$  are constant. With  $\mathbf{s}_t^a$  prescribed in (9),  $\gamma_1^a$  and  $\gamma_3^a$  are determined from (43)<sub>2</sub>. The boundary between the region A and region M is a  $c_3$  characteristic. This means that the discontinuity in  $\mathbf{s}_t^a$  and  $\mathbf{s}_t^m$  must be proportional to  $\mathbf{r}_3^a$ . Hence

$$\gamma_1^m = \gamma_1^a. \quad (44)$$

Equation (42) with the aids of (38) and (43)<sub>1</sub> has the expression

$$\rho V_1 \mathbf{u}^{1-} - \mathbf{s}^{1-} = \{(V_1/c_1^-)^2 - 1\} \gamma_1^m \mathbf{r}_1^a + \{(V_1/c_3^-)^2 - 1\} \gamma_3^m \mathbf{r}_3^a$$

and from (41) we obtain

$$\left. \begin{aligned} \gamma_1^a &= -\frac{(V_1/c_1^a)^2 + 3}{\{(V_1/c_1^a)^2 - 1\}^2} \left( \frac{\kappa_r}{V_1} \right) \gamma_1^0 = \gamma_1^m, \\ \gamma_3^m &= -\frac{(V_1/c_3^a)^2 + 3}{\{(V_1/c_3^a)^2 - 1\}^2} \left( \frac{\kappa_r}{V_1} \right) \gamma_3^0. \end{aligned} \right\} \quad (45)$$

Equation (45)<sub>1</sub> provides the initial acceleration  $\kappa_v$  of the shock wave  $V_1^*$ . Since  $\gamma_1^0$  is positive by (39),  $\kappa_v$  and  $\gamma_1^a$  have the opposite signs. In other words, the shock wave  $V_1^*$  grows when  $\gamma_1^a < 0$  and decays when  $\gamma_1^a > 0$ . For the  $s_t^a$  shown in Fig. 1,  $\gamma_1^a < 0$  and the shock wave  $V_1^*$  grows as indicated by the positive curvature of  $V_1^*$  in Fig. 3. The value of  $\gamma_3^a$  has no effects on the growth or decay of shock wave  $V_1^*$ .

If  $\gamma_1^a = 0$ ,  $\kappa_v = 0$  and  $s_t^m = \mathbf{0}$ . The wave pattern in the x-t plane is then given in Fig. 4 in which the region M is a constant state and the region A has a non-centered simple wave solution.

**7. Concluding remarks.** The example given in the last section illustrates how one can determine the growth or decay of a shock wave in the generalized Goursat-Riemann problem. The example was one of the simplest cases in which the two stress states  $s^a$  and  $s^b$  are on a shock wave curve  $V_1$ . Other simple cases have the two stress states on a shock wave curve  $V_3$  or on a simple wave curve  $c_1$  or  $c_3$ . For the latter, the discontinuity condition (24) for  $U^1$  will be needed. More complicated cases would have the two stress states at arbitrary locations in the stress space in which  $s^a$  can be reached from  $s^b$  through a series of simple wave curves and/or shock wave curves. More studies on the subject is being undertaken and results will be reported in the future.

**Acknowledgements** The work presented here is supported by the U.S. Air Force Office of Scientific Research under Contract AFSOR-89-0013.

#### REFERENCES

- [1] Yongchi Li and T. C. T. Ting, *Plane waves in simple elastic solids and discontinuous dependence of solution on boundary conditions*, Int. J. Solids Structures, **19** (1983), 989-1008.
- [2] Zhijing Tang and T. C. T. Ting, *Wave curves for the Riemann problem of plane waves in isotropic elastic solids*, Int. J. Eng. Sci., **25** (1987), 1343-1381.
- [3] C. Truesdell and W. Noll, "The Nonlinear Field Theories of Mechanics," Handbuch der Physik, Vol.III/3. Springer, Berlin (1965).
- [4] R. Courant and D. Hilbert, "Methods of Mathematical Physics," Vol.II. Interscience, New York (1962).
- [5] T. -P. Liu, *The Riemann problem for general  $2 \times 2$  conservation laws*, Trans. Amer. Math. Soc., **199** (1974), 89-112.
- [6] D. G. Schaeffer and M. Shearer, *The classification of  $2 \times 2$  systems of nonstrictly hyperbolic conservation laws, with application to oil recovery*, Appendix with D. Marchesin and P. J. Paes-Leme. Comm. Pure. Appl. Math., **40** (1987), 141-178.
- [7] M. Shearer, D. G. Schaeffer, D. Marchesin and P.J. Paes-Leme, *Solution of the Riemann problem for a prototype  $2 \times 2$  system of nonstrictly hyperbolic conservation laws*, Arch. Rat. Mech. Anal., **97** (1987), 299-320.

- [8] D. G. Schaeffer and M. Shearer, *Riemann problems for nonstrictly hyperbolic  $2 \times 2$  systems of conservation laws*, Trans. Amer. Math. Soc., **304** (1987), 267–306.
- [9] Guangshan Zhu and T. C. T. Ting, *Classification of  $2 \times 2$  nonstrictly hyperbolic systems for plane waves in isotropic elastic solids*, Int. J. Eng. Sci., **27** (1989), 1621–1638.
- [10] C. M. Dafermos, “Hyperbolic systems of conservation laws,” Brown Univ. Report, LCDS 83-5 (1983).
- [11] Xabier Garaizar, *Solution of a Riemann problem for elasticity*, J. Elasticity. (in press).
- [12] T. C. T. Ting and Tankin Wang, *The Goursat-Riemann problem for plane waves in isotropic elastic solids with velocity boundary conditions*, in IMA Volumes in Mathematics and Its Applications, **29**, James Glimm and Andrew J. Majda, eds., Springer-Verlag (1991), 367–386.
- [13] T. C. T. Ting, *The initiation of combined stress waves in a thin walled tube due to impact loadings*, Int. J. Solids Structures, **8** (1972), 269–293.
- [14] Ph. Le Floch and P. A. Raviart, *An asymptotic expansion for the solution of the generalized Riemann problem. Part 1: general theory*, Ann. Inst. H. Poincaré, Nonlinear Analysis. (in press).
- [15] A. Bourgeade, Ph. Le Floch and P. A. Raviart, *An asymptotic expansion for the solution of the generalized Riemann problem. Part 2: application to the equations of gas dynamics*, Ann. Inst. H. Poincaré. (in press).
- [16] T. C. T. Ting, *Further study on one-dimensional shock waves in nonlinear elastic media*, Q. Appl. Math., **37** (1980), 421–429.
- [17] T. C. T. Ting, *Intrinsic description of three-dimensional shock waves in elastic fluids*, Int. J. Eng. Sci., **19** (1981), 629–638.
- [18] Yongchi Li and T. C. T. Ting, *Lagrangian description of transport equations for shock waves in three-dimensional elastic solids*, Appl. Math. & Mech., **3** (1982), 491–506.
- [19] T. C. T. Ting and Yongchi Li, *Eulerian formulation of transport equations for three-dimensional shock waves in simple elastic solids*, J. Elasticity (1983), 295–310.
- [20] P. D. Lax, *Hyperbolic systems of conservation laws II*, Comm. Pure Appl. Math., **10** (1957), 537–566.